

ISTANBUL TECHNICAL UNIVERSITY ★ ENERGY INSTITUTE

**MODELING THE TEMPERATURE BEHAVIOR OF
THE GROUND SOURCE HEAT EXCHANGER SYSTEMS**



M.Sc. THESIS

Yousef GOLIZADEH AKHLAGHI

Energy Science and Technology Division

Energy Science and Technology Program

JUNE 2016

ISTANBUL TECHNICAL UNIVERSITY ★ ENERGY INSTITUTE

**MODELING THE TEMPERATURE BEHAVIOR OF
THE GROUND SOURCE HEAT EXCHANGER SYSTEMS**



M.Sc. THESIS

**Yousef GOLIZADEH AKHLAGHI
(301131053)**

Energy Science and Technology Division

Energy Science and Technology Program

Thesis Advisor: Assoc.Prof. Ömer İnanç TÜREYEN

JUNE 2016

İSTANBUL TEKNİK ÜNİVERSİTESİ ★ ENERJİ ENSTİTÜSÜ

**ZEMİN KAYNAK ISI DEĞİŞTİRİCİ SİSTEMLERİ
SICAKLIK DAVRANIŞ MODELLEMESİ**

YÜKSEK LİSANS TEZİ

**Yousef GOLIZADEH AKHLAGHI
(301131053)**

Enerji Bilim ve Teknoloji Anabilim Dalı

Enerji Bilim ve Teknoloji Programı

Tez Danışmanı: Doç. Dr. Ömer İnanç TÜREYEN

HAZİRAN 2016

Yusef GOLIZADEH AKHLAGHI, a M.Sc. student of ITU Energy Institute student ID 301131053, successfully defended the thesis entitled “**MODELING THE TEMPERATURE BEHAVIOR OF THE GROUND SOURCE HEAT EXCHANGER SYSTEMS**”, which he prepared after fulfilling the requirements specified in the associated legislations, before the jury whose signatures are below.

Thesis Advisor : **Assoc.Prof. Omer Inanc Tureyen**
Istanbul Technical University

Jury Members : **Prof.Dr.Altug Şişman**
Istanbul Technical University

Assoc. Prof. Hakan Demir
 Yıldız Technical University

Date of Submission : 2 May 2016
Date of Defense : 8 June 2016



To my Family,





FOREWORD

I would like to express my deep appreciation and thanks for my advisor, Prof.Omer Inanc Tureyen. This was impossible without his warm guidance, support and encouragement during the entire master study.

Special thanks to Prof.Abdurrahman Satman for his positive and helpful giudence during the study.

I would like to thank my friend Kagan Kutun for his kind and effective helps and guidance.

At the end, I would like to thanks my family for their warm support and love in my life.

June 2016

Yousef GOLIZADEH AKHLAGHI



TABLE OF CONTENTS

	<u>Page</u>
FOREWORD	vii
TABLE OF CONTENTS	ix
ABBREVIATIONS	xi
NOMENCLATURE	xiii
LIST OF TABLES	xv
LIST OF FIGURES	xvii
1. INTRODUCTION	1
1.1 Literature Review	1
1.2 Heat Pump	2
1.2.1 Overview	2
1.2.2 Air source heat pumps.....	6
1.2.3 Ground source heat pumps.....	8
1.2.3.1 Closed loop ground source heat pumps	11
1.2.3.1.1 Vertical.....	11
1.2.3.1.2 Horizontal.....	12
1.2.3.1.3 Pond or lake	13
1.2.3.1.4 Radial or directional drilling.....	14
1.2.3.2 Open loop.....	14
1.2.4 Statistics	15
1.2.4.1 World	15
1.2.4.2 Turkey	21
1.3 Scope Of Thesis	22
2. MATHEMATICAL MODEL	25
2.1 Ground Source Heat Exchanger System Model.....	25
2.2 Verification.....	31
3. EXAMPLE APPLICATIONS	37
3.1 Overview	37
3.2 Results	37
3.2.1 Radial	37
3.2.2 Cartesian.....	43
4. CONCLUSION	51
REFERENCES	53
CURRICULUM VITAE	55

ABBREVIATIONS

ASHP	: Air Source Heat Pump
ASHRAE Engineers	: American Society of Heating, Refrigerating, Air-Conditioning
COP	: Coefficient of Performance
EPA	: Environmental Protection Agency
GCHP	: Ground Coupled Heat Pump
GSHEs	: Ground Source Heat Exchanger Systems
GSHP	: Ground Source Heat Pump
GWHP	: Ground Water Heat Pump
HVAC	: Heating, Ventilating, Air Conditioning
ITU	: Istanbul Technical University
MTOE	: Million tonnes of Oil Equivalent
SCW	: Standing Column Well
SWHP	: Surface Water Heat Pump



NOMENCLATURE

Q	: Amount of transferred Heat
γ	: Conduction Index
A	: Cross Sectional Area
ρ	: Density of grid
d	: Distance Between the Grid Point
h	: Enthalpy
h	: Height of Grid
u	: Internal Energy
w	: Mass flow rate
Φ	: Porosity of grid
r	: Radius
C	: Specific Heat Capacity
T	: Temperature
t	: time
λ	: Thermal Conductivity
V	: Volume of grid
W	: Work done on the heat pump

Sub-indices:

b	: Borehole
g	: Grid point
H	: High temperature sink
inj	: Injection
L	: Low temperature source
m	: Matrix
p	: Production
i	: Represents grid
j_l	: Represents Neighboring grid
u	: U tube
w	: Water



LIST OF TABLES

	<u>Page</u>
Table 2.1: Properties of the system in verification.....	33
Table 3.1: Properties of the formation and of the borehole.	38
Table 3.2: Properties of the system for Cartesian system.	43





LIST OF FIGURES

	<u>Page</u>
Figure 1.1: Typical GSHP	3
Figure 1.2: Heat transfer fluid cycle.	4
Figure 1.3: Simple model of heat pump procedure (Sonntag, 1998).....	5
Figure 1.4: A heat pump can be used for heating or cooling(Cengel, 2007)..	6
Figure 1.5: Sample of Air Source heat pump.....	7
Figure 1.6: Small domestic ground source heat pump in home.....	9
Figure 1.7: Illustration of GSHP in both winter and summer.(EHPA, 2015).....	11
Figure 1.8: Vertical closed loop ground source heat pump(Banks, 2009).....	12
Figure 1.9: Horizontal closed loop ground source heat pump(Banks, 2009).	13
Figure 1.10: Pond or Lake closed loop ground source heat pump(Banks, 2009).	14
Figure 1.11: Open loop ground source heat pump(Banks, 2009).	15
Figure 1.12: Geothermal resource map of the United States (Boyd, 2015).....	16
Figure 1.13: Geothermal heat pump units installed in Canada from 1990 to 2013(Raymond, 2015).....	18
Figure 1.14: Distribution of geothermal heat pump systems (Raymond, 2015).....	19
Figure 1.15: Market development of HP in europ (EHPA, 2015).	20
Figure 1.16: Installed capacity of heat pumps in EU countries.(Efficiency, 2009)..	20
Figure 1.17: German heat pump market development (Efficiency, 2009).	21
Figure 1.18: Swedish heat pump market development (Efficiency, 2009).....	21
Figure 2.1: Schematics of the grid blocks used in the study(Akhlaghi, 2015).	25
Figure 2.2: Various types of u tube configurations considered in the study. a) Borehole with one u tube b) borehole with two u tubes (Akhlaghi, 2015).	26
Figure 2.3: Illustration of any grid i and the neighboring grids(Tureyen, 2009).....	27
Figure 2.4: Significantly large borehole grids (Red colors).....	33
Figure 2.5: Comparison of the analytical and numerical model(Akhlaghi, 2016). ..	34
Figure 2.6: Comparison of the analytical model temperature distribuion with numerical model for 10th day and 100th day(Akhlaghi, 2016).....	34
Figure 3.1: Schematic view of grid block in radial system.....	38
Figure 3.2: Temperature profile of outlet grid (production) for a circulation rate of 0.1 kg/s.....	39
Figure 3.3: Temperature profiles at the exit of the u-tube for various flow rates.	40
Figure 3.4: Temperature profile of the formation at the 100th day.	41
Figure 3.5: Temperature distibution for different initial values.....	42
Figure 3.6: Comparison of the production temperature with and without underground water flow for two different mass low rates.....	42
Figure 3.7: Areal logarithmic grid (Top view).	44
Figure 3.8: Areal logarithmic grid (Front view).	44

Figure 3.9: Temperature behavior around the well at 100th day for various flow rates.....46

Figure 3.10: Temperature profile around the well for different days and for constant flow rate.....47

Figure 3.11: Temperature distribution around the well.48

Figure 3.13: The temperature distribution for different formation thermal conductivities at 10th day.....49

Figure 3.14: The temperature distribution for different formation thermal conductivities at 100th day50



STUDYING TEMPERATURE BEHAVIOR OF GROUND SOURCE HEAT PUMP SYSTEMS

SUMMARY

Ground Source Heat Exchanger Systems (GSHEs) are becoming more popular everywhere in the world. GSHEs use pipes which are buried in the ground in order to extract heat from the ground. The heat can then be used to heat radiators, underfloor, swimming pools or to warm air heating systems and water in homes for several uses. Mixture of water and antifreeze circulates within the single or series of u tubes which are buried in the ground. Heat from the ground is absorbed by the circulating fluids and then by passes through a heat exchanger into the heat pump. The temperature of the ground remains approximately constant during the year.

There are several different factors influencing the performance of the GSHEs such as mass flow rate of circulating water, length of the u tubes, number of u tubes, number of boreholes, surface temperature, injection temperature, presence or absence of underground water flow, thermal conductivity of the fluid and formation, radius of u tube, radius of borehole, piping type, depth of operation, ground characteristics, capacity of heat pump system, size of system, building system, etc.

Mathematical models that are used for modeling the performance of the GSHEs are well established and have a significant role on studying the GSHEs. These models usually consider conductive heat transfer for the formation and the convective heat transfer for the fluid circulating within the u tube. Also convective heat transfer is considered for the underground water flow. Underground water flow is one of the most common factors which occurs inside the earth. It can have positive and negative effects on the performance of the GSHEs. Recently researchers have focused on studying the effect of underground water flows due to their significant effects.

In this study, we have developed a numerical model in order to study the effect of underground water flow. Our model is based on solving the energy balance equation. This equation is treated in fully implicit manner so that it becomes highly nonlinear. Hence, one numerical method must be used in order to overcome the nonlinearity. The Newton Raphson procedure is used in order to solve the equation.

Numerical derivatives are used in order to construct the Jacobian matrix. After solving the equation, in order to have trustable results we have verified our numerical model with one analytical model. In order to apply the same inputs and have the same situation in both numerical and analytical model or mimic the analytical model, we have to apply some simplicity in our numerical model.

For instance, because temperature distribution using geothermal gradient is not considered in the analytical model, it is taken to be zero. We have used several cases in order to make sure the verification is completed.

We have studied above-mentioned parameters in two radial and Cartesian systems. In the radial system we have studied the behavior of the produced water. Additionally, the effect of mass flow rate of the circulating water within the u tube have been studied. As a result, we saw that by increasing the mass flow rates from 0.01 to 100 kg/s the temperature profiles decline quickly to the value which is very close to the injecting water temperature that is 5°C in this study.

Furthermore, in the radial system, different initial temperatures have used in order to simulate the presence of underground water flow in the system. Since when underground water is present, it is normally cooler than the ground temperature. Mass flow rate of underground water flow is important too, so that the effect of mass flow rate of underground water is studied too. We have chosen two different mass flow rates in this case. Based on results, we saw that the effect of different initial temperature is significant.

In the Cartesian system we have studied the effect of underground water flow. In this case, forth layer is chosen to bear the underground water flow so that the temperature of this layer is assumed to be 15 °C. In this case, several mass flow rates are chosen for the underground water flow. Based on results we have concluded in the presence of underground water flow the temperature of the formation grids decrease less. This decrease become more efficient by increasing mass flow rate of the underground water. Furthermore, the overall increase for the temperature of the grid blocks can be seen due to the conductive heat transfer among the layers.

In the final step, we have studied the effect of thermal conductivity. Value of thermal conductivity is one of the crucial parameters that could have significant effects on the performance of GSHES which is very common in the actual systems. Three different thermal conductivities have been chosen for the formation. Based on results, for the lower thermal conductivities the borehole cools the most because of little amount of heat transfer among the borehole grids and formation grids.



TOPRAK KAYNAKLI ISI POMPALARININ SICAKLIK DAVRANIŐI

ÖZET

Toprak Kaynaklı Eőanör Sistemleri (GSHEs) gün geçtikçe daha çok kullanılıp popüler hale geliyor. GSHEs yerden ısı elde etmek amacıyla bahçede gömülü olan boruları kullanıyor. Çıkan ısı, radyatörleri ve yüzme havuzuları ısıtmak için kullanılabilir ya da hava ısıtma sistemleri ve su ısıtmak için kullanılabilir. Su ve antifriz karışımı toprağa gömülü U tüplerin içinde dolaşır ve yerden ısı dolaşım sıvıları tarafından emilir ve ısı pompası içine bir ısı dağıtıcısı boyunca geçer. Toprak sıcaklığı yıl boyunca yaklaşık olarak sabit kalır.

Termal olarak GSHEs performansını etkileyen çeşitli faktörler vardır. Dolaşım suyu kütle akış hızı, U tüpler uzunluğu, U tüplerin sayısı, sondaj kuyularına sayısı, yüzey sıcaklığı, enjeksiyon ısısı veya yeraltı su akışı, ısı iletkenlik oluşumu, U boru yarıçapı, sondaj kuyusu yarıçapı, boru tipi, işletme derinliği, yer özellikleri, ısı pompası sisteminin kapasitesi, sistemin boyutu ve inşaat sistemi bu faktörlerden bazılarıdır.

GSHEs performansını modellemek için kullanılan matematiksel modeller iyi sonuç vermiş ve GSHEs üzerinde önemli bir rolü vardır. Bu modeller genellikle U tüp içinde dolaşan akışkan için konvektif ısı transferini kullanıyorlar. Ayrıca ısı taşınımı yeraltı su akışı için kabul edilir. Yeraltı su akışı toprak içinde oluşur ve bu knudaki en yaygın faktörlerden biridir. Bu faktörün GSHEs performansı üzerinde olumlu ve olumsuz etkileri olabilir. Araştırmacılar son zamanlarda yeraltı su akımlarının önemli etkilerini incelemeye odaklanmışlardır.

Bu çalışmada, yeraltı su akışının etkisini araştırmak amacıyla bir sayısal model geliştirdik. Bizim modelimiz enerji dengesi denklemi çözmeye dayalıdır. Bu denklem tam kapalı bir şekilde işlemde geçirilir. Bu nedenle, bir sayısal yöntem lineer olmayan aşmak için kullanılmalıdır. Newton-Raphson prosedürü denklemi çözmek için kullanılır. Sayısal türev Jakobyen matris oluşturmak amacıyla kullanılmaktadır. Denklemi çözdükten sonra, güvenilir sonuçlar elde etmek için bir analitik model ile bizim sayısal modeli doğrulandı. Aynı girişleri uygulamak ve hem sayısal ve analitik modelde aynı sonuçları almak için, sayısal modelde bazı sadelik uygulamalar uyguladık. Jeotermal gradyanı kullanılarak, analitik sıcaklık dağılımı modeli olarak kabul edilir, Doğrulama tamamlandıktan emin olmak için birkaç vaka kullandık.

Biz iki radyal ve kartezyen sistemlerde parametreleri yukarıda bahsedilen durumda inceledik. Radyal sistemde ürettiğimiz suyun davranışını inceledik. Buna ek olarak, U boru içinde dolaşan suyun kütle akış oranının etkisi incelenmiştir. Sonuç olarak, 0.01 ila 100 kg arasında kütle akış oranlarını arttırarak, bu çalışmada 5°C olan enjekte su sıcaklığına çok yakın bir değere hızlı düşüşü görüldü.

Ayrıca, radyal sistem, farklı başlangıç sıcaklıkları sistemdeki yeraltı su akışının varlığını taklit etmek üzere kullanılmıştır. Yeraltı suyu zemin suyundan normak olarak daha soğuktur. Yeraltı suyunun kütle akış oranının etkisinin çok çalışılan böylece yeraltı su akışının kütle akış hızı, çok önemlidir. Biz bu durumda iki farklı kütle debileri seçtiniz. sonuçlarına dayanarak, farklı başlangıç sıcaklığının etkisinin çok büyük olduğunu gördüldü.

Kartezyen sistemde yeraltı su akışının etkisini inceledik. Bu durumda, ileri katmanlar bu tabakanın sıcaklığı 15 ° C olarak kabul edilir ve böylece altı suyu akışını taşımak için seçilir. Bu durumda, çok sayıda kütle akış hızları yeraltı suyu akışı için tercih edilmektedir. Sonuçlarına dayanarak biz oluşum ızgaraları sıcaklığı daha az azalma yeraltı su akışı varlığında sonucuna varmışlardır. Bu düşüş yeraltı suyu kütle akış hızını arttırarak daha verimli hale gelir. Ayrıca, ızgara blokları sıcaklığı genel bir artış katmanları arasında, iletken ısı aktarımı nedeniyle görülebilir.

Son aşamada, termal iletkenlik etkisini inceledik. Isı iletkenlik değeri gerçek sistemlerinde yaygındır ve GSHES performansı üzerinde önemli etkilere sahip olabilir önemli parametrelerden biridir. Üç farklı termal iletkenlikleri oluşumu için seçilmiştir. Sonuçlarına göre, düşük ısı iletkenlik için sondaj ızgaraları ve oluşum ızgaraları arasında ısı transferi çok az miktarda en etkilidir.





1. INTRODUCTION

1.1 Literature Review

Various studies exist in the literature regarding the modeling of such systems. The early studies model the system with the line source model. The temperature field for the line source solution is given by (Carslaw, 1959). The thermal response test used for estimating the thermal conductivity of the formation is given initially by (Choudhary, 1976) and (Morgensen, 1983). (Sanner, 2005) provides an overview of the Thermal Response Test. (Wang, 2010) developed a new test method for thermal response tests. In their study a novel constant heating temperature method is used for the thermal response test. It is shown that the proposed constant heating temperature method provides shorter test times when compared with conventional thermal response tests. As a result, thermal conductivity properties of the formation can be inferred using such a methodology. (Aydin, 2014) studied the long term performance prediction of a borehole. In their study, (Aydin, 2014) uses an analytical model and compares them with experimental data from the lab. They also consider determining the optimal time necessary for a thermal response test. (Gultekin, 2014) studied the optimal distance between boreholes for GSHEs. They have considered various configurations of borehole spacing. The above mentioned literature considers only the transfer of heat to / from the borehole to the formation via conduction. However, in most underground formations there exist water which could be mobile. In the presence of underground water flow, the heat exchange could be affected significantly depending on the rate of the underground water flow. (Signorelli, 2007) compared the results from a 3D finite element numerical model with those of a simple analytical line source solution and tested their sensitivity to the duration of the test. The effects of heterogeneous subsurface conditions and groundwater movements have also been considered. (Akhlaghi, 2015) uses numerical model to study the effect of underground water flow on the performance of ground source heat exchangers.

1.2 Heat Pump

1.2.1 Overview

A heat pump is a device that provides heat energy from a source of heat to a destination called a "heat sink". Heat pumps are designed to move thermal energy opposite to the direction of spontaneous heat flow by absorbing heat from a cold space and releasing it to a warmer one. A heat pump uses some amount of external power to accomplish the work of transferring energy from the heat source to the heat sink.

While air conditioners and freezers are familiar examples of heat pumps, the term "heat pump" is more general and applies to many HVAC (heating, ventilating, and air conditioning) devices used for space heating or space cooling. When a heat pump is used for heating, it employs the same basic refrigeration-type cycle used by an air conditioner or a refrigerator, but in the opposite direction, releasing heat into the conditioned space rather than the surrounding environment. In this use, heat pumps generally draw heat from the cooler external air or from the ground. In heating mode, heat pumps are three to four times more efficient in their use of electric power than simple electrical resistance heaters. Typically installed cost for a heat pump is about 20 times greater than for resistance heaters.

In the European Directives on the use of Renewable Energy , “Heat pumps enabling the use of aerothermal, geothermal or hydrothermal heat at a useful temperature level need electricity or other auxiliary energy to function. The energy used to drive heat pumps should therefore be deducted from the total usable heat. Only heat pumps with an output that significantly exceeds the primary energy needed to drive it should be taken into account.” (Sanner, 2003)

Heat pumps are generally more expensive to purchase and install than other heating systems in most of the countries around the world, but they can save money in the long period because of their lower bills. Although their initial installing price are high, but they are getting more and more popular among the customers. The statistics of heat pumps will be discussed later, but it is beneficial to know that approximately one-third of all single family homes built in the United States in the last decade are heated by heat pumps. (Lund, 2016)

Heat pumps consist of:

- Compressor
- Evaporator
- Condenser
- Expansion valve.

Figure 1.1 gives the structure of ground source heat pump system (GSHP) which will be described in details later. The water-antifreeze mixer which shown in blue color go inside the heat exchanger which is called evaporator here. Within the evaporator there is a refrigerant which acts as a heat transfer fluid. The heat is absorbed from the underground by the water-antifreeze mixer, transfer to the refrigerant inside the evaporator and causes it to boil and turns it to the gas. The refrigerant never physically mixes with the water-antifreeze mixer. They are separated by the plates of the heat exchangers which are shown on the figure. This gas then enter to the compressor which increase the pressure of the gas. The gas with high pressure and temperature which shown in red color flows into the second exchanger calls condenser and its heat transfers to the water which distributes the heat into the heating distribution system. Having transferred its heat, the refrigerant gas turns into liquid. This liquid passed through the expansion valve in order to reduce its temperature and pressure which is ready to commence the cycle all over again.

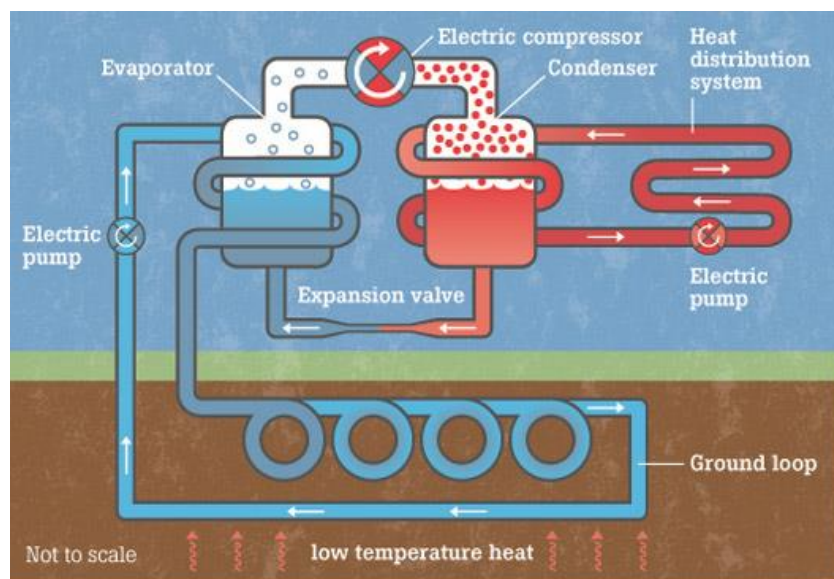


Figure 1.1: Typical GSHP (EHPA, 2015) .

Figure 1.2 gives the circulation of the heat transfer fluid in the heat pumps. The fluid starts the cycle with low pressure and low temperature. By passing the evaporator and absorbing the heat from the water-antifreeze mixer which was discussed in the Figure 1.1 it turns to low pressure vapor. It turns to be high pressure vapor by passing the compressor. Then it turns to high pressure liquid by losing the heat in the condenser. Finally it become ready to continue the cycle by reducing the pressure and temperature in expression valve.

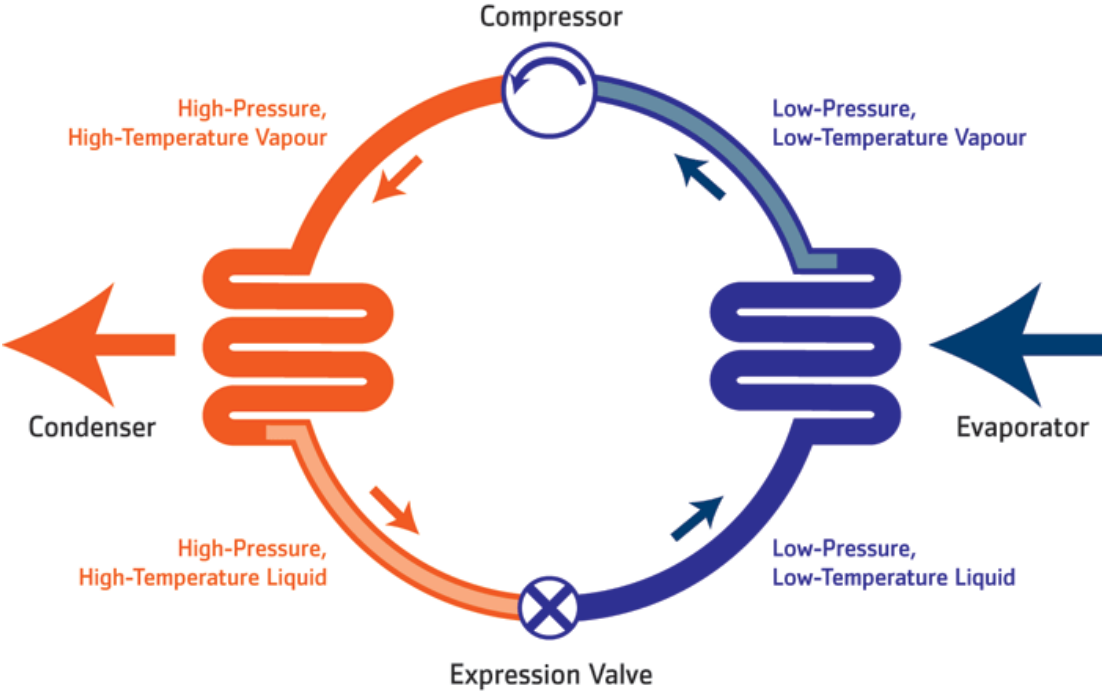


Figure 1.2: Heat transfer fluid cycle (EHPA, 2015).

Heat pumps models are usually described by simple structure. As shown in Figure 1.3 heat pumps work between two constant temperatures. Q_L is the heat which transfer from the low temperature source (T_L) to the heat pump. W is the work which is done on the heat pump such as the electricity that is needed for running the heat pump. Finally Q_H is the heat which transfers to the high temperature sink. The efficiency of the heat pumps is described by the coefficient of performance (COP) which is described by equation 1.1:

$$COP = \frac{Q_H}{Q_H - Q_L} = \frac{Q_H}{W} \tag{1.1}$$

COP is the ratio of the produced heat to the insereted work. The common energy sources for the heat pumps which separate the classifications of the heat pumps are atmospheric air, water and soil. The most common problem with

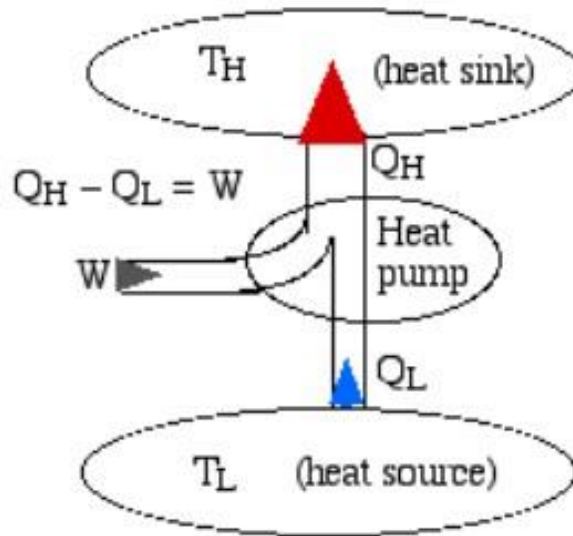


Figure 1.3: Simple model of heat pump procedure (Sonntag, 1998).

air-source heat pump systems is frosting, which occurs in humid climates, especially when the temperature falls below 2 to 5 °C. This frost prevents heat transfer through the evaporator coils so that the efficiency of the system reduces. The water source heat pumps use water and they do not have any frosting problem. They normally have higher COPs but they have other disadvantageous such as being complex and requiring easy access to a large body of water such as an underground water. The COPs of heat pumps usually varies between 1.5 and 4 depending on different factors such as temperature of ground water source and particular system used. The new improved heat pumps use variable-speed electric motor drives are at least twice as energy efficient as predecessors.

The efficiency of heat pump decreases significantly at low temperatures. Thus, majority of the air source heat pumps require supplementary heating systems such as electric resistance heaters or oil or water furnace in order to prevent from the temperature reduction. Since water and soil temperatures do not fluctuate much, supplementary heating may not be required for water-source or ground-source systems.

Heat pumps and air conditioners have the same mechanical components as mentioned Figure 1.4. Therefore, it is not logical and economical to have two separate systems in order to heating or cooling the building. One system can be used as a heat pump in winter and an air conditioner in summer. This is accomplished by

adding a reversing valve to the cycle. Figure 1.4 illustrates both heating and cooling mode. The condenser of the heat pump which is located inside acts as the evaporator of the air conditioner in summer and the evaporator of the heat pump which located outdoors acts as the condenser of the air conditioner. Thermodynamic heat pump cycles or refrigeration cycles are the conceptual and mathematical models for heat pumps and refrigerators that are listed below.

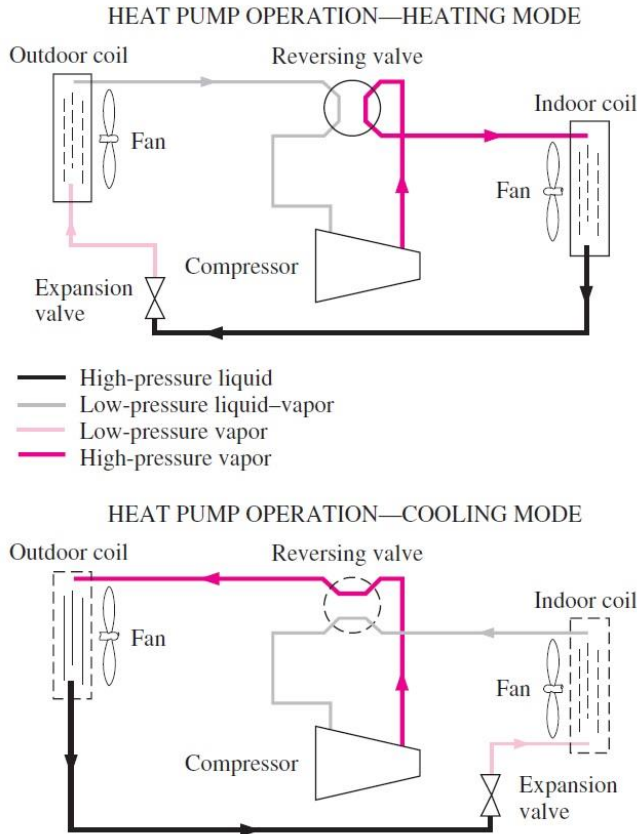


Figure 1.4: A heat pump can be used for heating or cooling (Cengel, 2007).

1.2.2 Air source heat pumps

As long as the temperature is above -18°C, enough heat can be drawn out of the surrounding air to heat your house. Air Source Heat Pumps basically take the air from the outside and convert it into heat that can be used to provide warmth for radiators or hot water tanks.

An Air Source Heat Pump (ASHP) normally fits to the outside of the house, either at the side or the back, and sucks in the air, using a mechanism to compress and increase its temperature. This can then be sent to under floor heating or radiators and

used to store hot water in a cylinder that can be utilized for showers, baths and the daily wash.

Unlike Ground Source Heat Pumps, air Source heat pumps (ASHP) don't require a large amount of construction works and most domestic units can be fitted quite easily. When the air enters the pump, it is absorbed at a low temperature in a fluid which is then compressed. This increases the temperature which is subsequently passed into the heating systems of the house. The air source heat pump system consists of an external box which is fitted to your outside wall as shown in Figure 1.5. It harvests renewable, low grade energy from the outdoor air and upgrades this into useful heat to supply a home with hot water and heating. For every 1kW of electricity fed into an heat pump unit (i.e.the outdoor part of the heating system), at least 3kW of heating energy is gotten. (Lund, 2004)



Figure 1.5: Sample of Air Source heat pump (EHPA, 2015).

There are two main types of Air Source Heat Pump:

Air to water systems: These send the heat to the water based units of your house such as the hot water tank or radiators. As with Ground Source Heat Pumps, these work better with things like under floor heating rather than traditional radiators because heat is produced at a lower temperature than normal gas central heating, for example.

Air to air system: This produces a flow of warm air that can be used to heat rooms and is circulated by fans. It is more limited than air to water and is not used to produce hot water or heating for radiators.

The Benefits of an Air Source Heat Pump:

- ✓ It could well lower the existing energy bills, for example if it is replaced with air source heat pump (ASHP).
- ✓ The carbon footprint would be reduced.
- ✓ Maintenance of the system is relatively cheap and can be used to heat entire the home.
- ✓ It's usually cheaper and have easier installing steps compared to GSHP.

1.2.3 Ground source heat pumps

In this study ground source heat pumps are assumed so that they will be explained more in detail. Ground source heat pumps or geothermal heat pumps (GSHP) which are also referred to as earth energy systems and Geo-Exchange systems have become commonplace almost everywhere as an heating and cooling applications. GSHP work by absorbing heat from the ground and transferring the absorbed heat into buildings in order to heat the buildings without using fossil fuels. They use the earth as a heat source in the winter or a heat sink in the summer. Ground source heat pumps can do all sorts of things from heating and cooling homes to warming swimming pools. These systems transfer heat by pumping water or a refrigerant (a special type of fluid) through pipes just below the Earth's surface, where the temperature is a constant 10 to 15°C. GSHPs are one of three categories of geothermal energy resources as defined by American Society of Heating, Refrigerating, and Air-Conditioning Engineers (ASHRAE) which are: high-temperature electric power production, intermediate and low-temperature. The GSHP are classified in low temperature group by operating relatively at low temperatures.

During the winter, the water or refrigerant absorbs warmth from the Earth, and the pump brings this heat to the building above. In the summer, some heat pumps can run in reverse and help cool buildings.

Figure 1.6 shows a small domestic ground source heat pump which is located inside the home.



Figure 1.6: Small domestic ground source heat pump in home (EHPA, 2015).

Although many parts of the country experience seasonal temperature, few feet below the earth surface the ground remains at a relatively constant temperature. Depending on latitude, ground temperatures range from 7°C to 21°C . Like a cave, this ground temperature is warmer than the air above it during the winter and cooler than the air in the summer. GSHP systems rely on the fact that, under normal geothermal gradients of about $30^{\circ}\text{C}/\text{km}$ (Thomas, 1982), the earth temperature is roughly constant in a zone extending from about 6.1m deep to about 45.7m deep. This constant temperature interval within the earth is the result of a complex interaction of heat fluxes from above (the sun and the atmosphere) and from below (the earth interior). As a result, the temperature of this interval within the earth is approximately equal to the average annual air temperature. Above this zone the earth temperature is a damped version of the air temperature at the earth's surface. Below this zone the earth temperature begins to rise based on the natural geothermal gradient. GSHP takes advantage of this by exchanging heat with the earth through a ground heat exchange.

GSHP systems consist of three loops or cycles. The first loop is on the load side and is either an air/water loop or a water/water loop, depending on the application. The second loop is the refrigerant loop inside a water source heat pump. Thermodynamically, there is no difference between the well-known vapor-compression refrigeration cycle and the heat pump cycle; both systems absorb heat at a low temperature level and reject it to a higher temperature level. The difference

between the two systems is that a refrigeration application is only concerned with the low temperature effect produced at the evaporator, while a heat pump may be concerned with both the cooling effect produced at the evaporator as well as the heating effect produced at the condenser. In these dual-mode GSHP systems, a reversing valve is used to switch between heating and cooling modes by reversing the refrigerant flow direction. The third loop in the system is the ground loop in which water or an antifreeze solution exchanges heat with the refrigerant and the earth.

The GSHP working procedure is summarized in 5 steps by regarding Figure 1.7 for both winter and summer seasons:

1. Water or a refrigerant is injected in to the ground through a loop of pipes which are located inside the ground in order to circulate the water.
2. When the weather is cold, the water or refrigerant heats up by gaining heat from the ground which has higher temperature than the water as it travels through the part of the loop.
3. Once it gets back above ground, the warmed water or refrigerant transfers heat into the building using the heat distribution facilities which are not shown in the figure
4. The water or refrigerant cools down after its heat is transferred to the building. Then it is reinjected to underground in order to heats up once more and to start the process again.
5. On a hot day or summer seasons the system can run in reverse. The water or refrigerant cools the building and then is pumped underground where extra heat is transferred to the ground around the pipes. In this cycle warm water which is absorbed the building heat is injected to the ground in order to loose its heat to the ground which is cooler than the water. Then the cooled water is transferred to the building in order to cool the building using the heat distribution systems. Finally after absorbing the heat of building it is reinjected to the ground in order to continue the process. Efficiency of GSHP is much greater than conventional air-source heat pump systems. A higher coefficient of performance (COP) can be achieved by a GSHP. Since as

mentioned before the source or the sink earth temperature is relatively constant compared to air temperature.

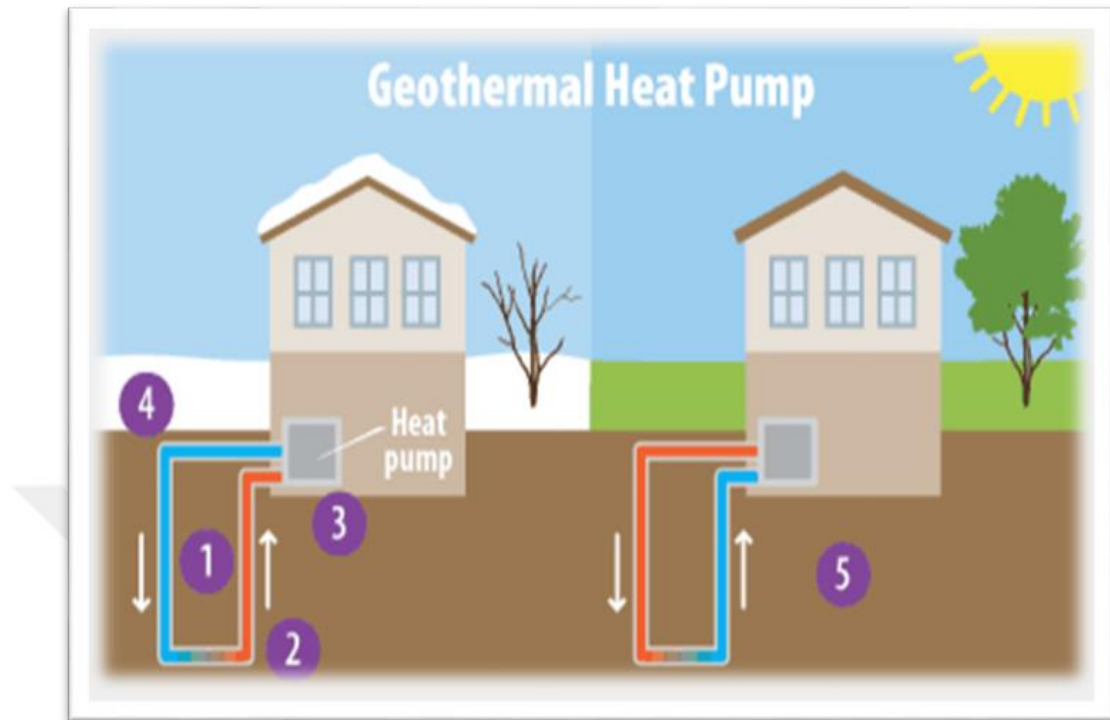


Figure 1.7: Illustration of GSHP in both winter and summer. (EHPA, 2015)

There are several classifications for the ground source heat pumps. In this section the most common categories will be discussed. These general categories are: 1. Closed loop GSHP and 2. Open loop GSHP.

1.2.3.1 Closed loop ground source heat pumps

In this type the water or antifreeze liquid is circulated in the closed loop system which is buried underground. In the closed loop GSHP systems heat transfers between the refrigerant in the heat pump and the liquid circulated in the pipes. In this type the loop can have different configurations:

1.2.3.1.1 Vertical

A vertical closed loop heat pump system is composed of pipes that is located vertically in the ground as it can be seen in Figure 1.8. Vertical closed loop GSHP systems are typically used when there is a limited area of land available. The system is buried at the depth of approximately 20 meter to 120 meter. For instance, a house needing 10 kW of heating capacity might need three boreholes 80 to 110 m deep.

The cost of digging is approximately high but after installing the system and when the system starts operation there is no need to any further interventions anymore. Pipes in the borehole connected each other with a U-shaped connector. The size and the number of boreholes and pipes can be different according to the ground type and amount of energy that is needed. Borehole is filled with some kind of grout which provide a high thermal connection between the pipes and soil or rock around them in order to improve heat transfer operation. The grout also protect the installed system from flooding and can prevent the underground water from contamination.

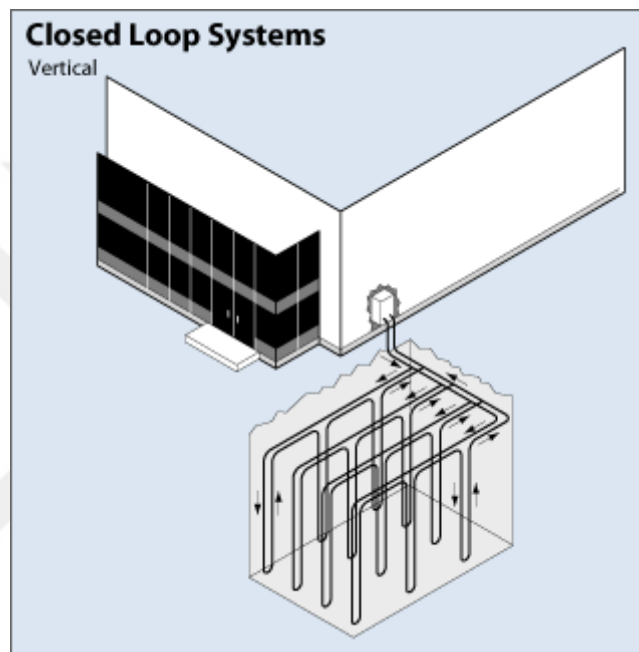


Figure 1.8: Vertical closed loop ground source heat pump (Banks, 2009).

1.2.3.1.2 Horizontal

Horizontal ground source heat pump systems are composed of pipes that are located horizontally in the ground. The cost of excavation for horizontal GSHP systems are approximately half the cost of vertical drilling so that horizontal systems are commonly used in the residential systems and wherever there is enough place for installation the system. The most important advantages of this type is that it can be used in driveways and gardens without disturbing them.

The depth of system depends on the amount of energy that is needed and used by the heat pump. Usually one or two pipes are buried at the depth of 1 to 3 m. For instance the house needing 10 kW energy three pipes with 120 to 180 length are needed to be buried at the depth of 2 m.

Two main problems exist for the closed loop horizontal GSHP: 1) Shallow pipes tend to get warm by absorbing heat from the sun which can be a positive effect, especially when the ground is still cold after the winter. 2) In the cold periods when there is a high demand for heat, shallow pipes tend to get cold rapidly. So the cost of operation significantly increases. In order to overcome these problems the depth of system and the length of pipes should increase so that the cost of installation will increase. But it is logical because of high reduction in the cost of operation. Some recent researches indicate that using the non-homogeneous soil profile can solve the problem. Using the layer of soil with lower conductive material above the pipes can decrease the negative effect of shallow systems. Tests show that using this method increase the heat extraction from the ground by the 17% in the cold periods and approximately by the 6% in the warm periods which are high achievement in the engineering.

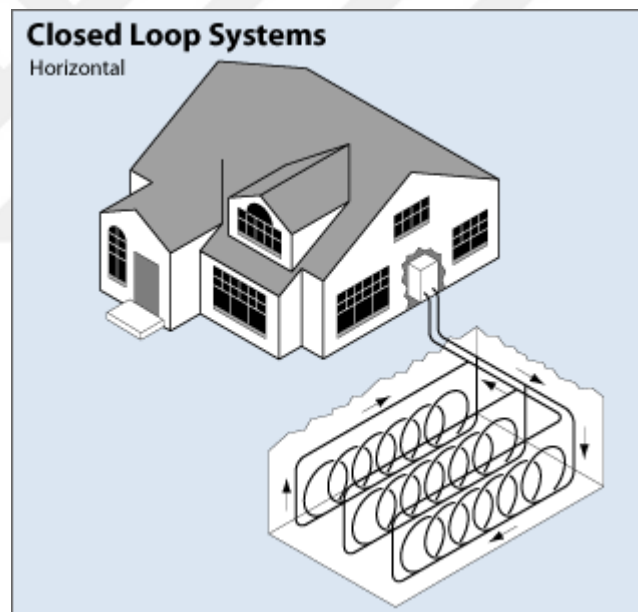


Figure 1.9: Horizontal closed loop ground source heat pump (Banks, 2009).

1.2.3.1.3 Pond or lake

The pipes locate in a spiral form on the bottom of the pond. It is important that the pipes place 2-5 meter beneath the water's freezing layers in the winter. Usually the pond distance from the home should not exceed 100 m and the area of water reservoir or pond should be greater than 200 square meters.

The most important advantages of this type is that there is no need to any excavation. There is low initial investment needed in this type and also the efficiency is high

enough. It is the best cost-effective type of ground source heat pump system to install and operate a geothermal energy. But the disappointing disadvantageous is that the lakes deeper than 2 meter can't be found everywhere which limits the installation of this type.

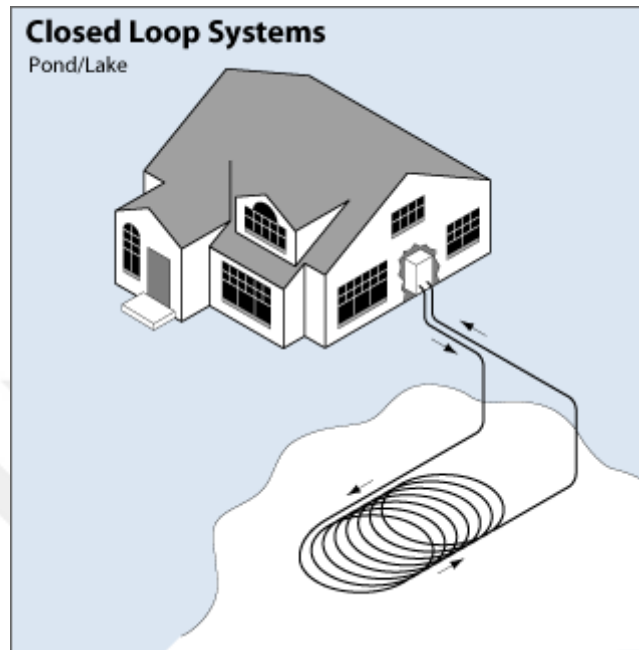


Figure 1.10: Pond or Lake closed loop ground source heat pump (Banks, 2009).

1.2.3.1.4 Radial or directional drilling

As an alternative to trenching, loops may be laid by mini horizontal directional drilling (mini-HDD). This technique can lay piping under yards, driveways, gardens or other structures without disturbing them, with a cost between those of trenching and vertical drilling. This system also differs from horizontal & vertical drilling as the loops are installed from one central chamber, further reducing the ground space needed. Radial drilling is often installed retroactively (after the property has been built) due to the small nature of the equipment used and the ability to bore beneath existing constructions.

1.2.3.2 Open loop

Open loop ground source heat pump is also called ground water heat pump (GWHP). As mentioned in the beginning the temperature at depth of 10-15m under the surface is approximately constant so that it is cooler than the outside in the summer and warmer than the outside in the winter. This natural advantage is used in the GWHP systems. GWHP systems can be installed near the groundwater sources in order to

benefit from the mentioned natural temperature difference. Heat is added or extracted from the ground water by primary refrigerant loop for the cooling and heating demands respectively, then used water is reinjected to the ground by separated injection well. It would be better to control the used water chemistry in order to prevent from the corrosion the materials or use the protected materials in the system.

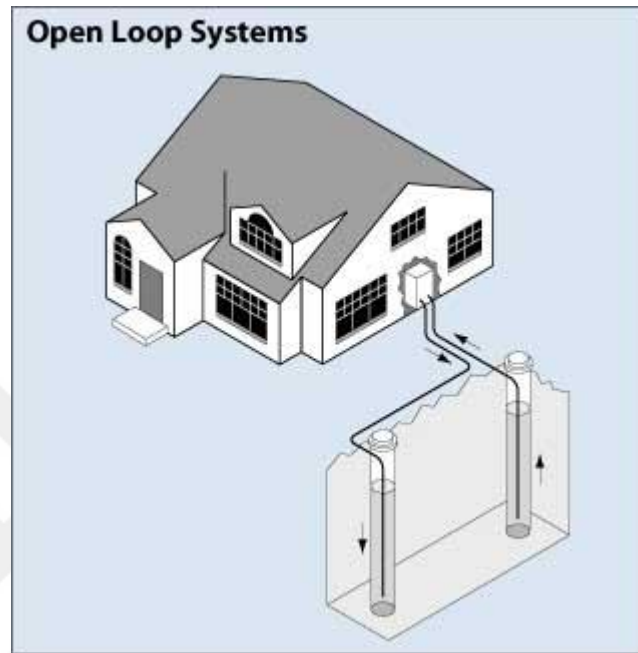


Figure 1.11: Open loop ground source heat pump (Banks, 2009).

1.2.4 Statistics

1.2.4.1 World

In this section the statistics of heat pumps will be discussed, however there is no any official report for the heat pumps. But in this study ground source heat pumps are important so that I try to focus on them.

Geothermal heat pumps (GSHP) strengthen U.S energy security. Every 100000 homes with geothermal heat pump systems reduce foreign oil consumption by 2.15 million barrels annually and reduce electricity consumption by approximately 800 million kilowatt hours annually (Efficiency, 2009). The GSHP systems are efficient enough. The use of geothermal lowers electricity demand by approximately 1kW per ton of capacity. United States Environmental Protection Agency (EPA) found that geothermal heating and cooling systems can reduce energy consumption and emissions by more than 40% compared to air source heat pumps and by over 70% compared to electric resistance heating with standard air conditioning equipment.

The feedbacks show that more than 95% of geothermal heat pump customers recommend the mentioned system to the other customers.

Geothermal heat pumps save money, for instance, schools now using geothermal heat pump systems save more than \$25 million in energy costs that it means this amount of money can be used in order to improve educational systems instead of energy utilization. Furthermore, homeowners can save 25 to 50 percent on home electric bills compared to conventional heating and cooling systems. Electrical bills for a 2000 ft² home can be reduced at least \$1 per day by using the geothermal heat pumps.

As it can be seen in Figure 1.12 there are lots of suitable areas especially in the western United States, where most of the recent volcanic and mountain building activity have occurred for installing the GSHP in the US.

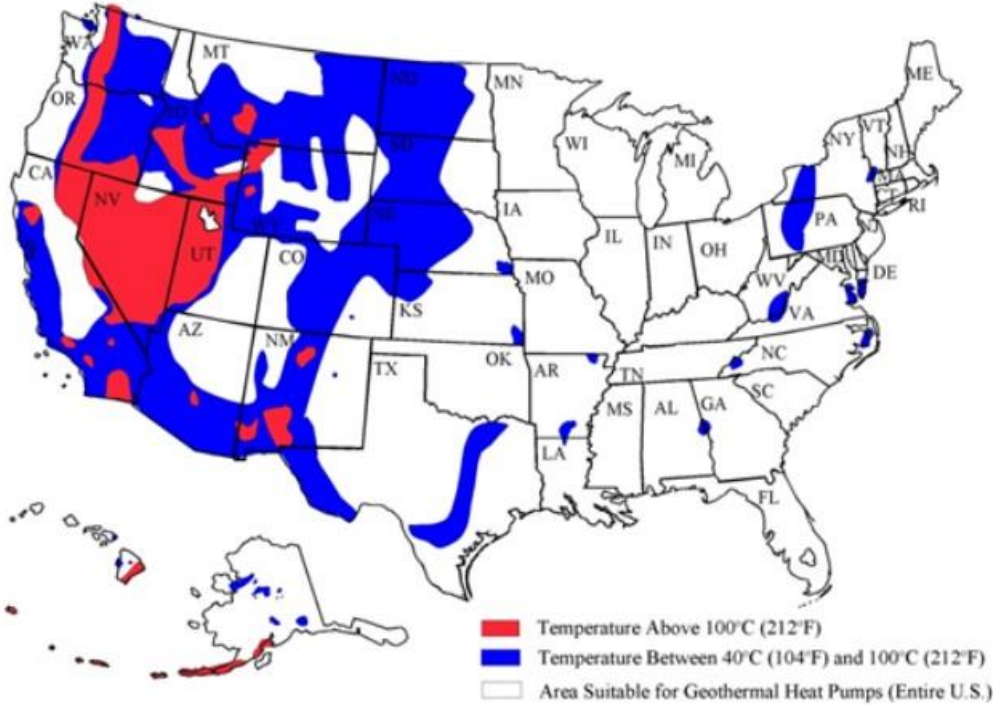


Figure 1.12: Geothermal resource map of the United States (Boyd, 2015).

Even though the actual number of installed units is difficult to determine, the present estimate is that there are at least 1.4 million units installed, mainly in the mid-western and eastern states. Of these approximately 60% of the units are installed in residences and the remaining 40% in commercial and institutional buildings. The current trend is that most of the newer units are being installed in commercial institutional buildings (60%) and only 40% in residential locations. Approximately

90% of the units are closed loop (ground-coupled) and the remaining open loop (water-source). Within the residential sector, of the closed loops systems, approximately 30% are vertical and 70% horizontal, as the latter are cheaper to install. In the institutional and commercial sector, 90% are vertical and only 10% horizontal, constrained by ground space in urban area (Boyd, 2015). By the mentioned amount of using geothermal heat pump systems the following emission reductions had resulted:

- Elimination of more than 5.8 million metric tons of CO₂ annually
- Elimination of more than 1.6 million metric tons of carbon equivalent annually.

These 1000000 installations have also resulted in the following energy consumption reductions:

- Annual savings of nearly 8 million kWh
- Annual savings of nearly 40 trillion Btus of fossil fuels.
- Reduced electricity demand by more than 2.6 million kW.

The monumental impact of the current use of geothermal is equivalent to:

- Taking close to 1295000 cars off the road
- Planted more than 385 million trees.
- Reducing U.S. reliance on imported fuels by 21.5 million barrels of crude oil per year.

The EPA has identified ground source heat pumps as a technology that significantly can reduce greenhouse gas and other air emissions associated with heating, cooling and water heating residential buildings alongside saving money. For every 100000 units of typically sized residential geothermal heat pumps installed, more than 37.5 trillion Btu's of energy used for space conditioning and water heating can be saved, corresponding to an emissions reduction of about 2.18 million metric tons of carbon equivalents, and cost savings to consumers of about \$750 million over the 20 year life of the equipment. EPA found that, even on a source field basis - accounting for ALL losses in the field circle including electricity generation at power plants - geothermal systems are much more efficient than competing fuel technologies. They

are an average of 48% more efficient than the best gas furnaces on a source fuel basis, and over 75% more efficient than oil furnaces. In fact, today best geothermal systems outperform the best gas technology, gas heat pumps, by an average of 36% in heating mode and 43% in cooling mode. The U.S. general Accounting Office estimates that if geothermal systems were installed nationwide, they could save several billion dollars annually in energy costs and substantially reduce pollution.

Figure 1.13 gives the total number of installed GSHP in the Canada from 1990 to 2013. The number of units installed is for both the residential and commercial sectors and units of the commercial sector have been expressed in equivalent residential units, taking into account the heat pumps capacity. The industry experienced a growth rate of 40% during 2006 to 2008 and severely decreased from 2010 to 2012. Peak installation of 15913 units occurred in 2009. The most recent data obtained for 2013 suggested that installations were roughly half of those reported for 2009. High growth rates before 2009 is explained by the increase of oil prices, the relatively high prices of natural gas with peaks in 2005 and 2008. The 2010 downturn is thought to be due to the 2009-2010 financial crisis, the decrease in oil and gas prices, the end of many government incentive programs, the increase of electricity prices and the loss of Canadian heat pump manufacture.

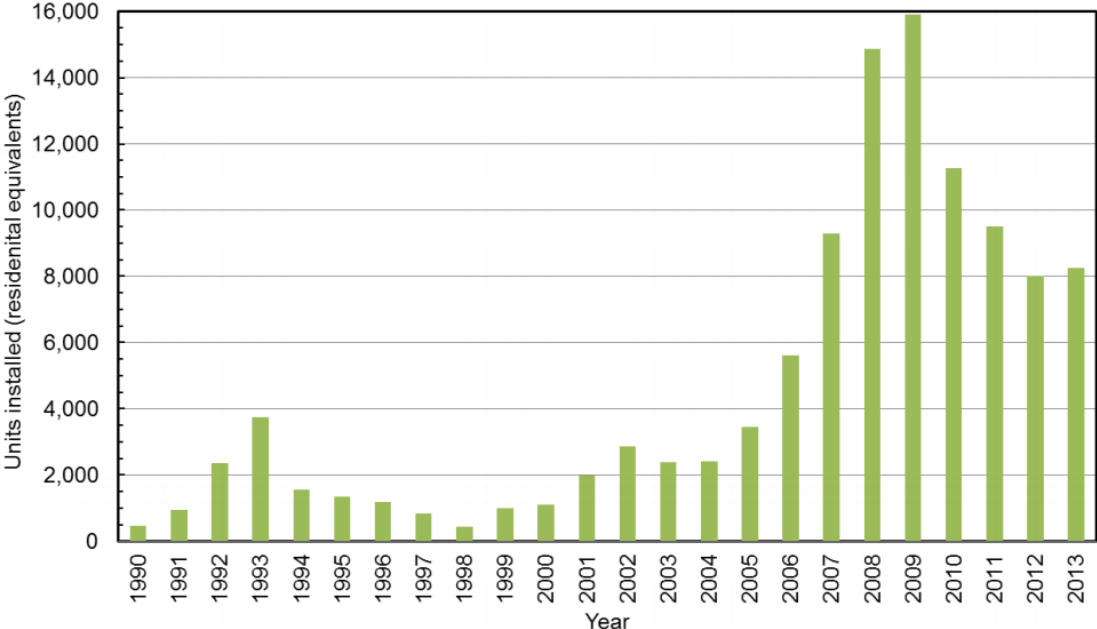


Figure 1.13: Geothermal heat pump units installed in Canada from 1990 to 2013 (Raymond, 2015).

The calculation indicates an annual geothermal energy used related to heating with geothermal heat pumps equal to 11111 TJ/yr for the end of 2013. This exploitation of shallow geothermal resources which is shown in Figure 1.14 is concentrated in southern Ontario and Quebec but present throughout the country, as evidenced by the map of geothermal heat pump systems.

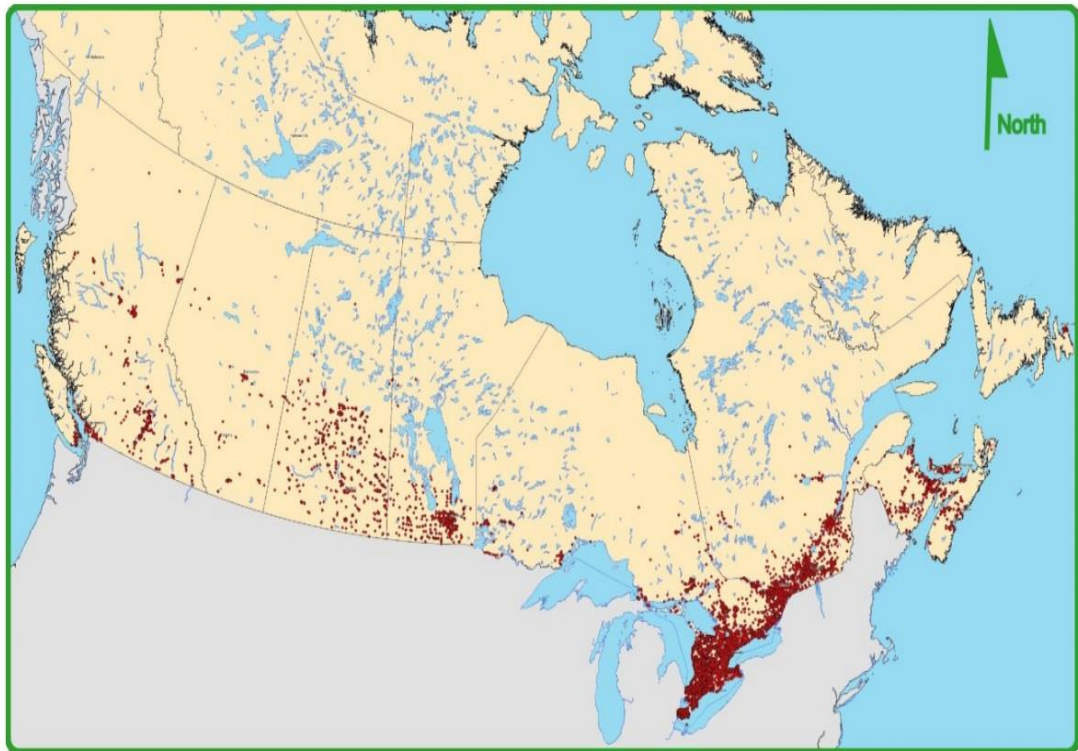


Figure 1.14: Distribution of geothermal heat pump systems (Raymond, 2015).

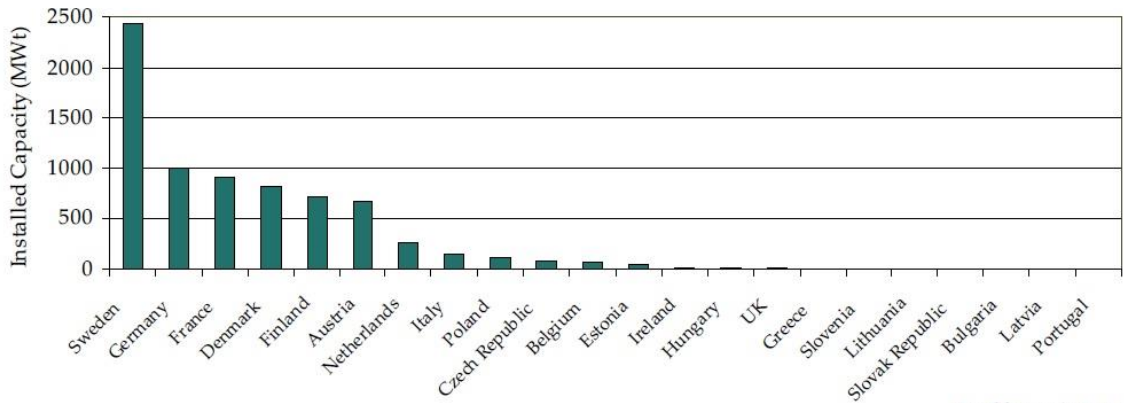
Figure 1.15 shows the heat pump market in European countries from 2006 to 2014. Red colors indicate the decrease and green colors indicate the increase in the markets. The overall increase can be seen in the Europe for heat pump markets.

As shown on Figure 1.16 the most popular countries for installing the GSHP systems are Germany and Sweden. So you can see the heat pump market developing in both countries in Figure 1.17 and Figure 1.18



Figure 1.15: Market development of HP in europ (EHPA, 2015).

European GSHP Installed Capacity



EurObserv'ER 2007

Figure 1.16: Installed capacity of heat pumps in EU countries. (Efficiency, 2009)

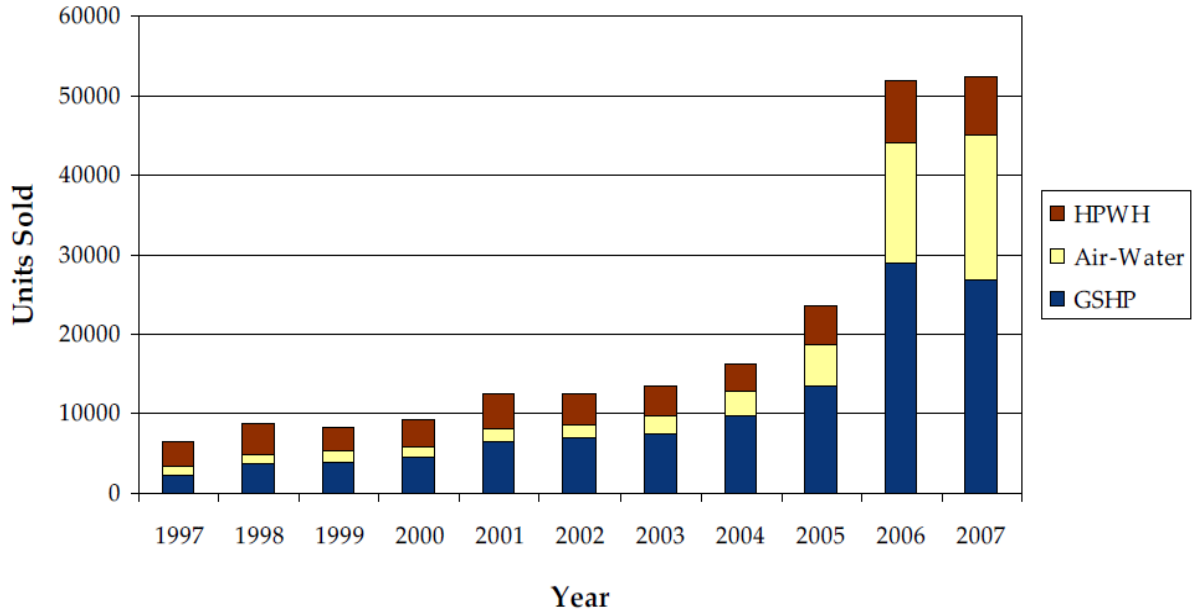


Figure 1.17: German heat pump market development (Efficiency, 2009).

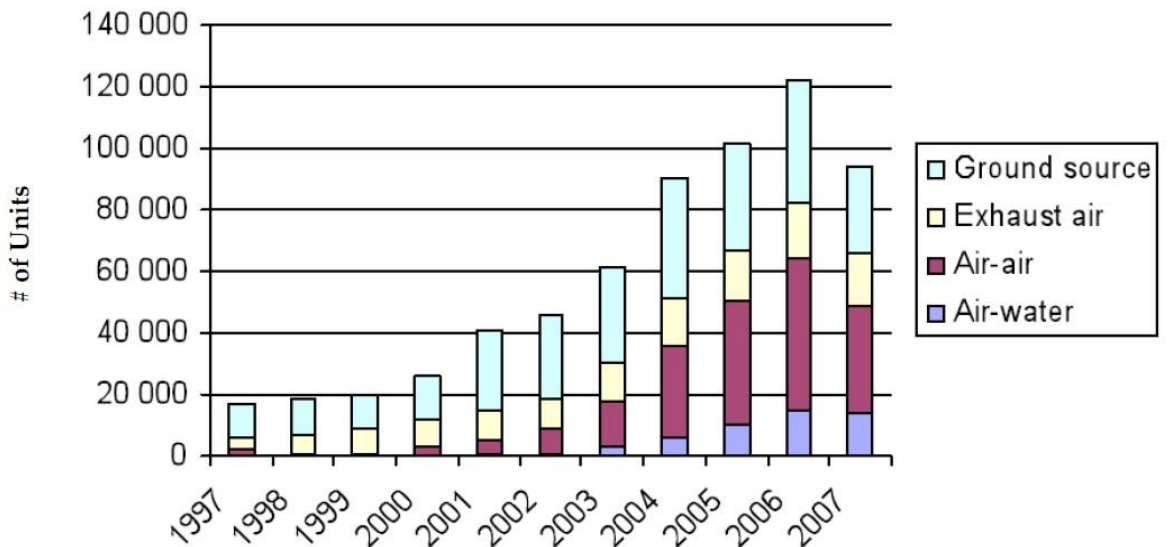


Figure 1.18: Swedish heat pump market development (Efficiency, 2009).

1.2.4.2 Turkey

Depending on Turkish HVAC industry committee statistics; about 44000 heat pump sold in Turkey market between 2013-2014. Turkey has been in the forefront of direct use application and development in recent years. Ground source heat pumps have been used in residential buildings for heating and cooling for approximately more than 15 years in Turkey .

The first residential geothermal heat pump system in the country was installed in a villa with a floor area of 276 m² in Istanbul, in 1998, while the first experimental study was carried out in the Mechanical Engineering Department, METU.

1.3 Scope Of Thesis

The current chapter was an introduction of this thesis. As it mentioned in the previous sections the heat source of GSHP is ground. The heat is taken from the ground by a borehole heat exchanger which has different types such as u-tube, helical shaped etc. The main purpose of this thesis is studying the temperature behavior of the GSHP. This aim became possible by developing the numerical model which are very popular and well established in studying the GSHP.

Next chapter includes the model that is based on solving the energy balance equation. The system which is simulated includes a single borehole that is located in the center of the system, a single u-tube which is located inside the borehole in order to circulate the fluid and finally the formation. Temperature distribution of the system is applied using the geothermal gradient which can be chosen regarding the cases. Temperature and mass flow rates of circulating fluid, the dimensions of the system such as radius of borehole and u-tube, depth of the ground, width of the field, surface temperature which has a significant role on the temperature distribution of the system, presence of underground water flow and its mass flow rate, etc can be applied using the model. Besides introducing the model, the verification is placed at the end of the chapter. The model is verified with an analytical model. Two cases used in order to verify the model. The first one represents the temperature behavior of the specific grid during the operation and the second case represents the temperature behavior of the system at two different days.

The third chapter includes the results. The results are given for two radial and cartesian systems. As it mentioned in the first chapter several factors influence the performance of GSHP. In the radial case we have focused on the mass flow rate of circulating water. The several mass flow rates for circulating water have been chosen in this section in order to study the effects of it. Furthermore, the different initial temperature is applied to the system in order to simulate the underground water flow and see the effects of it on the performance of the GSHP. In the cartesian system the effect of underground water flow has been focused. In this section several mass

flow rates are chosen and the results are given in the figures. Additionally, at the end of chapter the heterogeneity is studied. Several thermal conductivities have been chosen for the formation grids and the results are given in two figures.

The final chapter includes the conclusions. In this chapter the results are classified in order to conclude the thesis and organize the results.





2. MATHEMATICAL MODEL

2.1 Ground Source Heat Exchanger System Model

In this section, before going to mathematical model I am going to describe schematic of grid blocks that are given in Figure 2.1. As you see same discretization has been used for both borehole grids and formation grids in the vertical direction. Furthermore, the u-tube grids are located inside the well blocks that are separated by the bold line from the formation grids. It is important to note that the number of grid blocks in both horizontal and vertical directions are chosen just for describing the schematics of grid blocks.

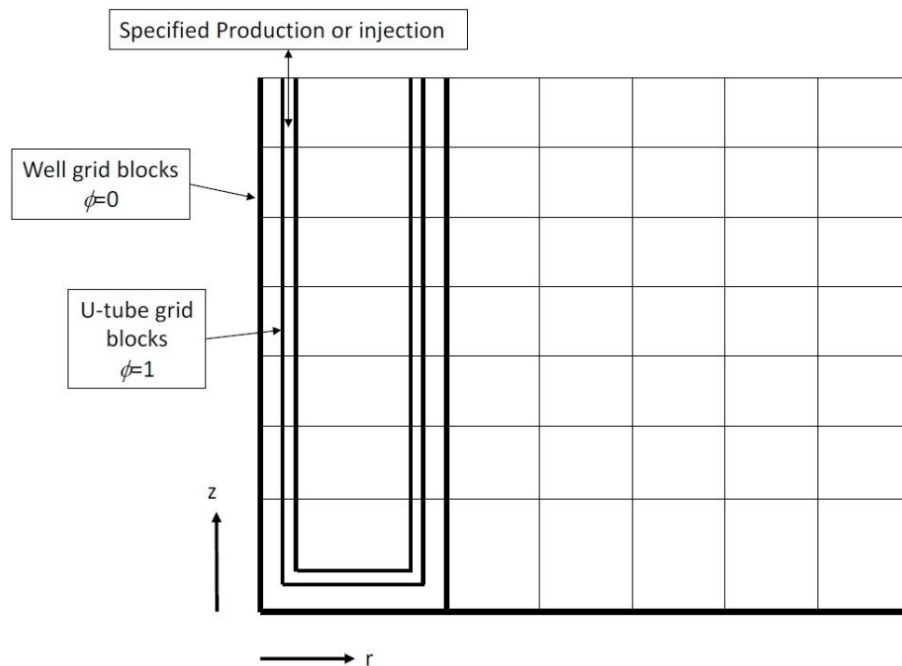


Figure 2.1: Schematics of the grid blocks used in the study (Akhlaghi, 2015).

Energy transfer among the u-tube grids is by way of conduction and convection. Energy transfer among the u-tube grids and the bore grids are by way of conduction only because there is now any fluid or water between mentioned grids and also energy transfer between the borehole grids and the formation grids are by way of conduction only for the same reason. Finally, energy transfer among the formations

grids is by way of conduction and also by way of convection in the presence of underground water flow which is very crucial for us in this study because of studying the effect of underground water flow.

As it can be seen on the Figure 2.1 porosity for the u tube grids is assumed to be one because of being fully water and zero for the borehole grids because there is no water inside the borehole grids. In some cases two u tubes can be used in order to continue the operation when one of the u tubes fails. Figure 2.2 illustrates two different configuration discussed here.

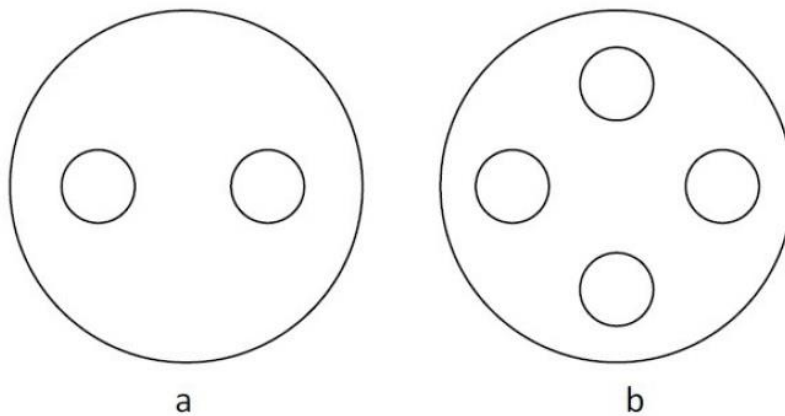


Figure 2.2: Various types of u tube configurations considered in the study. a) Borehole with one u tube b) borehole with two u tubes (Akhlaghi, 2015).

Our mathematical model based on solving the energy balance equation assuming steady state flow. The structure of the model is very similar to which developed by Tureyen and Akyapi (2011). Here we don't use mass balance equation. As mentioned, this model is developed based on energy conservation for a single phase fluid (here water). Then the equation is solved numerically by the Newton Raphson method after discretization on all tanks.

Here let's consider any grid i which can make an arbitrary number of connections with any other grid in the system which can be borehole, u-tube or formation grid. Figure 2.3 illustrates tank i and its properties. As it is clear on the figure the tanks are assumed to be composed of water and rock. Grid i has bulk volume of V_{bi} (m^3), porosity of ϕ_i and temperature of T_i ($^{\circ}C$). Grid i can make an arbitrary number of connections with neighboring grids which are represented by j_l with the specific mass flow rate of $w_{i,jl}$ (kg/s). Furthermore, grid i have an injection term by the specific

mass flow rate of $w_{inj,i}$ (kg/s) and temperature of $T_{inj,i}$ (°C) and production term with the specific mass flow rate of $w_{p,i}$ (kg/s) and the temperature of grid T_i (°C).

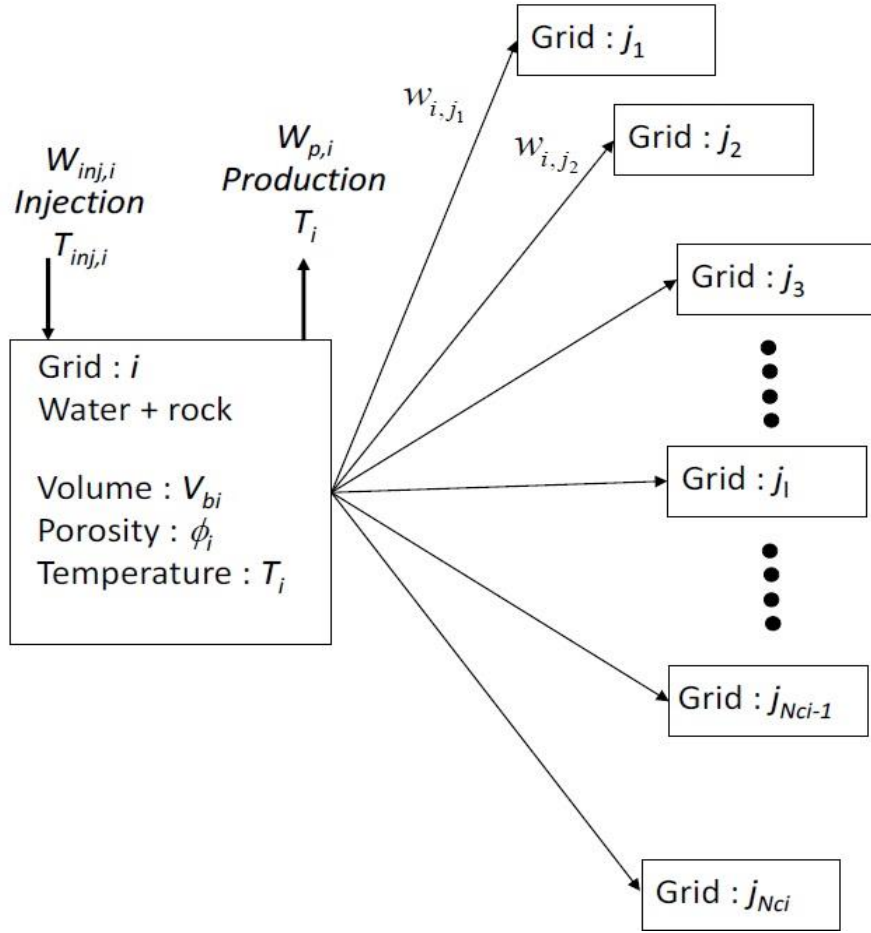


Figure 2.3: Illustration of any grid i and the neighboring grids (Tureyen, 2009).

Equation 2.1 illustrates the energy balance equation that is applied for grid i in this study.

$$\begin{aligned} \frac{d}{dt} [(1-\phi_i)V_i\rho_{m,i}C_{m,i}T_i + V_i\phi_i\rho_{w,i}u_{w,i}] + w_{inj,i}h_{w,inj,i} + w_{p,i}h_{w,i} - \sum_{l=1}^{N_{c,i}} w_{i,j_l}h_{\xi} \\ - \sum_{l=1}^{N_{c,i}} \gamma_{i,j_l}(T_{j_l} - T_i) \end{aligned} \quad (2.1)$$

Here as mentioned above V_i is the bulk volume, ϕ_i is the porosity and T_i is the temperature for grid i . Furthermore, u is the internal energy (J), C is the specific heat capacity (J/kg.°C), w is the mass flow rate (kg/s), h is the enthalpy (J/kg) and γ is the conduction index (J/s.°C). The sub-indices m , w , inj , and p represent the matrix, water, injection and production respectively. Total number of grids represented by N_c . The first term is the accumulation of energy in grid i . The second term represents

the energy contribution from injection, the third term represents the energy contribution from the production, the fourth term represents the energy contribution to and from neighboring grids and fifth term accounts for the contribution of energy from neighboring blocks by way of conduction.

An upwinding scheme is applied to the convective heat transfer among those grid blocks which heat transfer among them is by the way of convective. The subscript ξ represents the direction of upwinding and is defined by the following equation;

$$\begin{aligned} \xi &= i, \text{ if flow is from } i \text{ to } j_l \\ \xi &= j_l, \text{ if low is from } j_l \text{ to } i \end{aligned} \quad (2.2)$$

The descritization should preforme in time. For simplicity let's consider equation 2.3:

$$A = [(1 - \phi_i)V_i\rho_{m,i}C_{m,i}T_i + V_i\phi_i\rho_{w,i}u_{w,i}] \quad (2.3)$$

Now equation 2.1 can be written as below:

$$\frac{dA}{dt} + w_{inj,i}h_{w,inj,i} + w_{p,i}h_{w,i} - \sum_{l=1}^{N_{e,i}} w_{i,jl}h_{\xi} - \sum_{l=1}^{N_{e,i}} \gamma_{i,jl}(T_{jl} - T_i) = 0 \quad (2.4)$$

The energy balance equation is treated in a fully implicit manner causing it to become highly non-linear. Equation 2.5 shows the discretized form which a fully implicit scheme is applied for the equation 2.4:

$$\begin{aligned} \frac{A^{n+1} - A^n}{\Delta t^{n+1}} + w^{n+1}_{inj,i}(t)h^{n+1}_{w,inj,i}(T_{inj,t}) + w^{n+1}_{p,i}(t)h^{n+1}_{w,i}(T_i,t) - \sum_{l=1}^{N_{e,i}} w^{n+1}_{i,jl}h^{n+1}_{\xi} \\ - \sum_{l=1}^{N_{e,i}} \gamma^{n+1}_{i,jl}(T^{n+1}_{jl} - T^{n+1}_i) = R_i = 0 \end{aligned} \quad (2.5)$$

And it should be clear that:

$$\Delta t^{n+1} = t^{n+1} - t^n \quad (2.6)$$

Furthermore, it should be mentioned that the γ is treated to be constant during the study, hence we have equation 2.7:

$$\gamma^{n+1} = \gamma \quad (2.7)$$

Since equation (2.5) is highly nonlinear, Hence a Newton Raphson procedure is used to solve it. Hence, the following system of equations in the newton raphson method are needed to be solved:

$$\mathbf{J}^{n+1,k} \delta^{n+1,k} = -\mathbf{R}^{n+1,k} \quad (2.8)$$

Which \mathbf{R} is the residual matrix in the newton raphson method. For constructing the Jacobian matrix in the Newton Raphson procedure (\mathbf{J}), numerical derivatives are used. The jacobian matrix is given in equation 2.9:

$$\mathbf{J}^{n+1,k} = \begin{bmatrix} \frac{\partial R_1^{n+1,k}}{\partial T_1} & \frac{\partial R_1^{n+1,k}}{\partial T_2} & \dots & \frac{\partial R_1^{n+1,k}}{\partial T_{N_c}} \\ \frac{\partial R_2^{n+1,k}}{\partial T_1} & \frac{\partial R_2^{n+1,k}}{\partial T_2} & \dots & \frac{\partial R_2^{n+1,k}}{\partial T_{N_c}} \\ \dots & \dots & \dots & \dots \\ \frac{\partial R_{N_c}^{n+1,k}}{\partial T_1} & \frac{\partial R_{N_c}^{n+1,k}}{\partial T_2} & \dots & \frac{\partial R_{N_c}^{n+1,k}}{\partial T_{N_c}} \end{bmatrix} \quad (2.9)$$

$$\delta^{n+1,k} = \begin{bmatrix} \delta_1^{n+1,k} \\ \delta_2^{n+1,k} \\ \dots \\ \delta_{N_c}^{n+1,k} \end{bmatrix} \quad (2.10)$$

Here it is important to mention that:

$$\delta^{n+1,k+1} = T^{n+1,k+1} - T^{n+1,k} \quad (2.11)$$

$$\mathbf{R}^{n+1,k} = \begin{bmatrix} R_1^{n+1,k} \\ R_2^{n+1,k} \\ \dots \\ R_{N_c}^{n+1,k} \end{bmatrix} \quad (2.12)$$

Initialization of the vectors will be performed as below:

$$T^{n+1,0} = T^n \quad (2.13)$$

A forward difference scheme is used to handle the derivatives with respect to time.

$$\frac{\partial R_i}{\partial T_j} = \frac{R_i(T_j + \varepsilon) - R_i(T_j - \varepsilon)}{2\varepsilon} \quad (2.14)$$

As converge criteria both absolute and relative criteria can be used as follow:

$$\text{Absolute: } \max \delta_i^{n+1,k+1} \leq \beta \quad (2.15)$$

$$\text{Relative: } \max \frac{\delta_i^{n+1,k+1}}{T_i^{n+1,k+1}} \leq \beta \quad (2.16)$$

Where β can be different based on the problem criteria.

The conduction index can be computed as a function of thermal conductivity of the system. For neighboring two grid blocks in Cartesian coordinates the conduction index can be written as a function of thermal conductivity as follows:

$$\gamma_{i,j_i} = \left(\frac{\lambda A}{d} \right)_{i,j_i} \quad (2.17)$$

Here $A(\text{m}^2)$ is the cross sectional area between the grid blocks, $d(\text{m})$ is distance between the grid points and $\lambda (\text{J/m.s.}^\circ\text{C})$ is the thermal conductivity of the medium. It should be noted again that Equation 2.17 is given for grid blocks that neighbor each other in the Cartesian coordinate system. It is possible to write the conduction index for various other coordinate systems as a function of the thermal conductivity. Harmonic averaging is applied to the thermal conductivity in determining the conduction index.

Energy transfer by way of conduction only take places between the borehole grids and u tube grids so that it is highly important in this study. Since, here the approximation that is used in this study among the mentioned grids is described:

$$\gamma = \frac{\pi h \lambda r_u (r_b + r_u)}{r_o (r_o - r_u)} \quad (2.18)$$

Here $r_u(\text{m})$ is the radius of the U-tube, $r_b(\text{m})$ is the radius of the borehole, $h(\text{m})$ is the height of the grid. r_o is given by the following relationship:

$$r_o = \frac{r_b + r_u}{2} \quad (2.19)$$

Equation 2.18 is obtained using discretization of the diffusion equation in radial coordinates around the well. The assumption here is that the u tube is assumed to be at the center, where as on the real case it is slightly off center as shown in figure 3.1 and 3.2.

The conduction index between the borehole and the formation depends on the coordinate system. If a radial coordinate system is discretized, the conduction index can be determined as follows:

$$\gamma = \frac{\pi h \lambda r_w (r_b + r_w)}{r_g (r_g - r_w)} \quad (2.20)$$

where r_b (m) is the outer boundary radius of the grid block adjacent to the well and r_g (m) is the grid point of the same block. If discretization is carried out on Cartesian coordinates, the borehole is placed at the center of a square or a rectangle. For the conduction index between the borehole and the well, the following relation can be used:

$$\gamma = \frac{2\pi h \lambda}{\ln\left(\frac{r_e}{r_w}\right)} \quad (2.21)$$

where r_e (m) can be determined as follows:

$$r_e = 0.14\sqrt{\Delta x^2 + \Delta y^2} \quad (2.22)$$

where Δx (m) and Δy (m) are the lengths of the grid block bearing the borehole in the x and y directions respectively.

2.2 Verification

Before going to results, in this section two different cases have been used in order to verify the numerical model that is used in this study. Analytical model by (Aydin, 2014), is used for the verification. The following dimensionless equation is considered for the verification.

$$\theta(\tilde{r}, \tilde{t}) = \frac{-2}{\pi} \int_{\beta=0}^{\infty} \frac{e^{-\beta^2 \tilde{t}} [J_0(\beta \tilde{r}) Y_0(\beta) - Y_0(\beta \tilde{r}) J_0(\beta)]}{\beta (J_0^2(\beta) + Y_0^2(\beta))} d\beta \quad (2.23)$$

Where, θ is the dimensionless temperature, J is the Bessel functions of the first kind and Y is the Bessel function of the second kind. Dimensionless boundary and initial conditions which are assumed for solving the main equation to be:

$$\begin{cases} \theta(1, \tilde{t}) = 0 \\ \theta(\tilde{r}, 0) = 1 \\ \theta(\infty, \tilde{t}) = 0 \end{cases} \quad (2.24)$$

where \tilde{r} is the dimensionless radius, \tilde{t} is the dimensionless time.

The relationship among the dimensionless and dimensional factors are:

$$\begin{cases} T = \theta(T_\infty - T_b) + T_b \\ r = \tilde{r} r_b \\ t = \frac{\tilde{t} r_b^2}{\alpha} \end{cases} \quad (2.25)$$

Here T_∞ is initial temperature of the formation, T_b is temperature of the borehole wall, r_b is radius of the borehole and α is thermal diffusivity defined by $\alpha = \lambda / \rho c_p$, λ is the thermal conductivity and ρ is density of the ground and c_p is heat capacity of fluid. Equation 2.23 and Dimensionless boundary and initial conditions are provided using following conduction heat transfer equation in cylindrical system and dimensional boundary and initial conditions(Ozisik, 1993) :

$$\frac{\partial^2 T}{\partial r^2} + \frac{1}{r} \frac{\partial T}{\partial r} = \frac{1}{\alpha} \frac{\partial T}{\partial t} \quad (2.26)$$

$$\begin{cases} T(r_b, t) = T_b \\ T(r_b, 0) = T_\infty \\ T(\infty, t) = T_\infty \end{cases} \quad (2.27)$$

In order to apply the constant initial temperature for the borehole during the operation, volume of the borehole grids in the numerical model are assumed to be sufficiently large. This basically causes the temperature in the borehole grid blocks to be constant with time, hence the constant boundary condition can be reached by this method. These grid blocks are shown in Figure 2.4 in red color.

Furthermore, the analytical model assumes a constant temperature for the formation grids. In order to mimik this condition, the geothermal gradient is not considered in the initial temperature distribution in numerical study. The properties of system which is used in this section is given in Table 2.1.

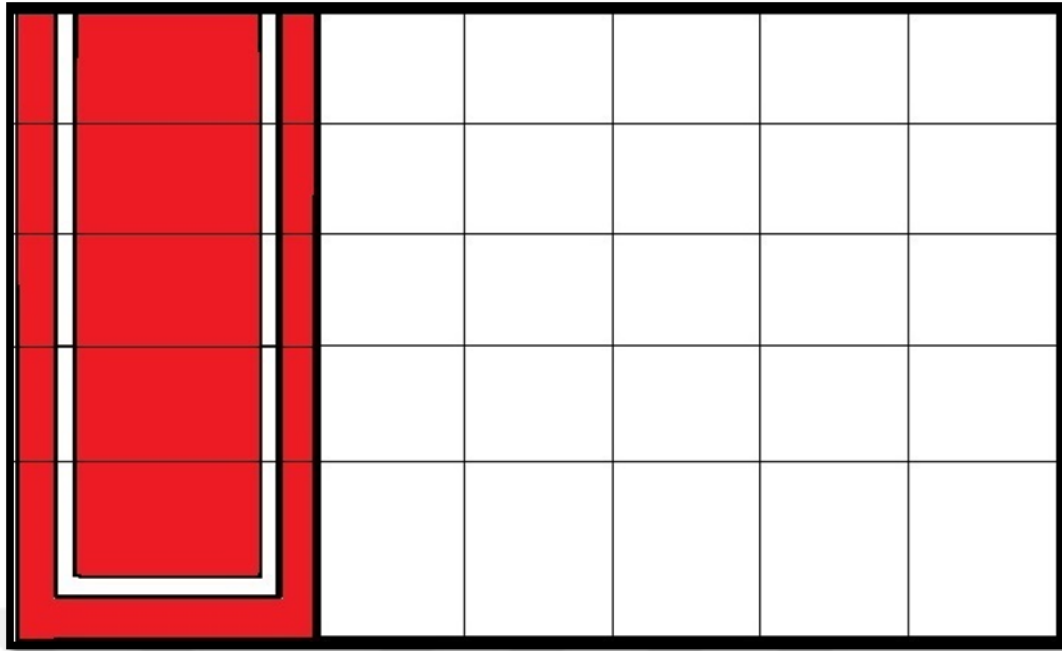


Figure 2.4: Significantly large borehole grids (Red colors).

Table 2.1: Properties of the system in verification.

Parameters	Quantity
Initial temperature of the formation, °C	20
Temperature of borehole, °C	15
Radius of borehole, m	0.2
Thermal conductivity of formation, J/(m.s.C)	2.92
Thermal conductivity of water, J/(m.s.C)	0.6
Density of ground, kg/m ³	2650
Heat capacity of formation, J/(kg.C)	1000
Outer radius of formation, m	1000
Duration of operation, D	100
Total depth of HSHES in numerical study, m	100
Total number of grids in numerical study	256
Number of grid block in r direction	40
Number of grid block in z direction	5
Radius of u-tube, m	0.02
Geothermal gradient in numerical study, C/m	0

Figure 2.5 gives the temperature behavior of a specific grid point during the operation which is located at approximately 0.42 m from the borehole center. As can be seen from Figure 2.5, the behavior of the temperature starts from the initial value. Since the temperature behavior given in Figure 2.5 is the behavior at formation

block, heat is transferred among the grids is only by way of conduction and the temperature starts to decrease. It is seen that the numerical profile is perfectly overlap with the analytical one.

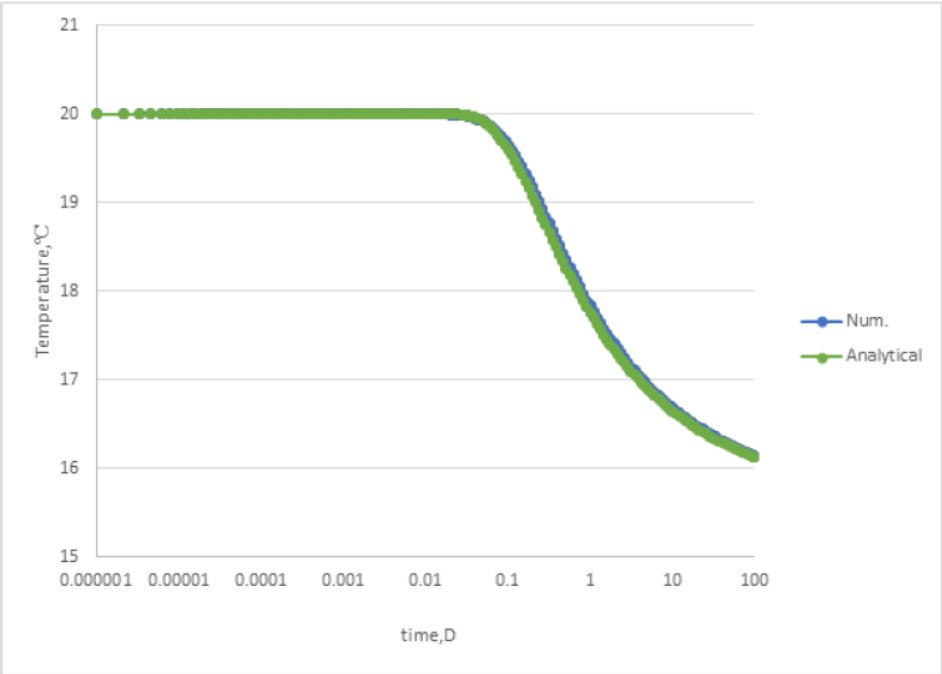


Figure 2.5: Comparison of the analytical and numerical model (Akhlaghi, 2016).

The second case that is used for the verification is shown in Figure 2.6.

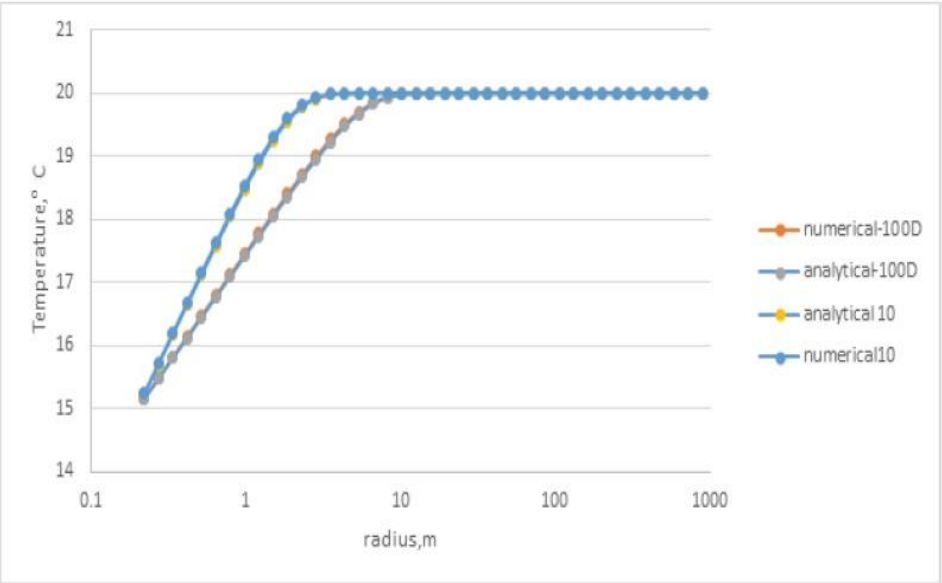


Figure 2.6: Comparison of the analytical model temperature distribuion with numerical model for 10th day and 100th day (Akhlaghi, 2016).

Figure 2.6 gives the temperature profiles for 10th day and 100th day. As it is clear, the total effected area for both 10th day and 100th day is around the borehole. As it can be seen when fluid is circulated in the U-tubes, heat will be extracted away from the formation near the wellbore as it expected. It is seen that the numerical profile is perfectly overlap with the analytical one in this case too. Hence the verification of the system is done.in the next chapter the results will be discussed.





3. EXAMPLE APPLICATIONS

3.1 Overview

In this chapter various synthetic applications will be described in order to study the behavior of GSHES. We have used two radial and cartesian systems in order to investigate the behavior of GSHPS. In every applications some kind of differences are used. Here are the main factors influencing the performance of GSHES which is studied in this chapter:

- Mass flow rates for injecting water
- Presence of underground water flow
- Thermal conductivity of the formation

In this study we have focused on some factors such as different mass flow rates for injecting fluid, different mass flow rates for underground water flow and different thermal conductivity for the formation which are common important factors influencing the performance of GSHES.

3.2 Results

3.2.1 Radial

In this case a discretized radial grid has been used. In this case the borehole located at the center. Figure 3.1 shows the grids which are used in the radial case. It is the front view of the system where the borehole, u-tube inside the borehole and the formation is obvious.

The properties of the GSHES for this radial case is listed below in Table 3.1 . this table includes all the properties which are constant for all radial cases which will be discussed in this chapter. The variable factors such as mass flow rate of circulating water is not listed in the table. Furthermore, any change in the listed properties will be mentioned anywhere needed.

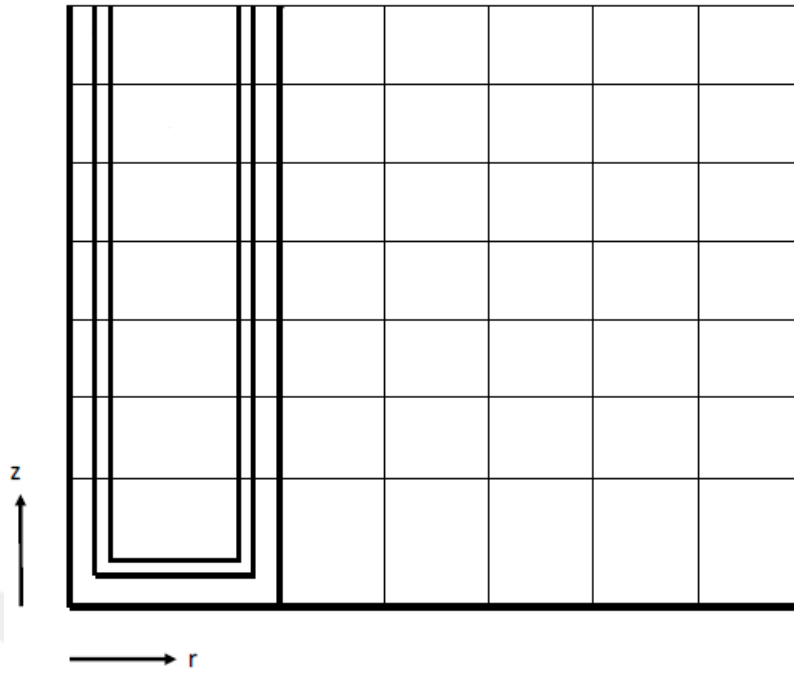


Figure 3.1: Schematic view of grid block in radial system.

Table 3.1: Properties of the formation and of the borehole.

Parameters	Quantity
Surface temperature, °C	20
Radius of borehole, m	0.2
Thermal conductivity of formation, J/(m.s.°C)	2.92
Thermal conductivity of borehole, J/(m.s.°C)	2.92
Thermal conductivity of water, J/(m.s.C)	0.6
Density of rock, kg/m ³	2650
Heat capacity of formation, J/(kg.C)	1000
Outer radius of formation, m	1000
Duration of operation, D	100
Total depth of HSHES in numerical study, m	100
Number of grid block in r direction	40
Number of grid block in z direction	5
Geothermal gradient in numerical study, C/m	0.033

A mass flow rate of 0.1 kg/s is used at first for circulating the water in the U-tube. The injected water is assumed to be at 5°C. Figure 3.2 gives the temperature behavior of the water produced from the U-tube. It is important to note that initially the temperature distribution within the U-tube, the borehole and the formation have been assigned using the geothermal gradient given in Table 3.1.

As can be seen from Figure 3.2, the behavior of the temperature starts from the initial value corresponding to the one obtained from the geothermal gradient. Since the temperature behavior given in Figure 3.2 is the behavior at the exit block of the U-tube, the temperatures of the grids below this point are at higher temperatures initially because of the geothermal gradient. Hence, when flow starts, there is an initial increase in temperature. As the cold water displaces the fluid, the temperature starts to decrease. Once the initial injected water is produced at the other end of the U-tube, the conduction dominated period starts and a straight line decrease in temperature is observed.

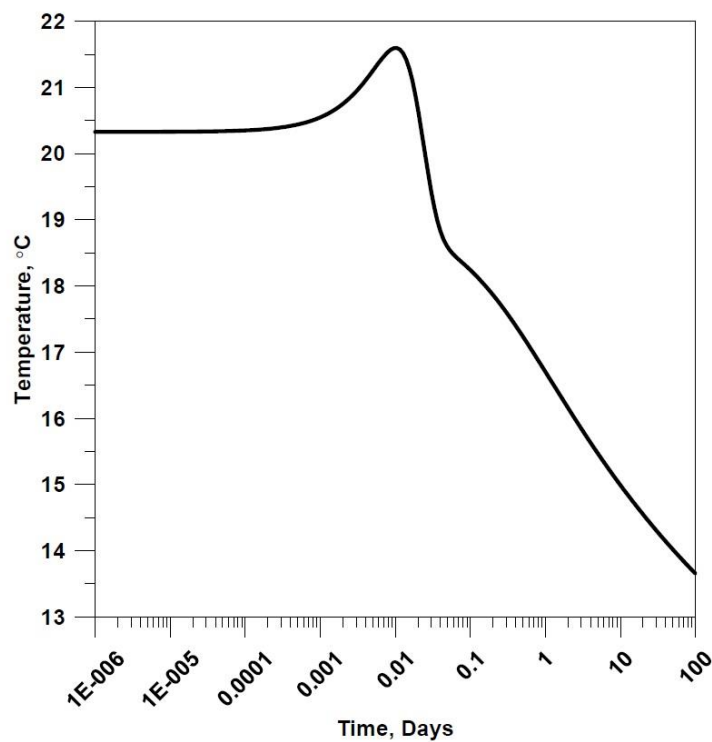


Figure 3.2: Temperature profile of outlet grid (production) for a circulation rate of 0.1 kg/s.

In the next step the effect of mass flow rates for the circulating water has been studied. The mass flow rates that are used in this step are: 0.01, 0.1, 1, 10 and 100 kg/s. As shown in results which are given in the Figure 3.3 with lower flow rates such as 0.01 kg/s, a similar behavior which is shown in Figure 3.2 is obtained except the decline rate of profile is decreased. As shown in the figure by increasing the mass flow rate, the temperature decline rate is increased too. For the high mass flow rates such as 100kg/s the temperature decline quickly to the value which is very close to the injecting temperature which here is 5°C. this is normally logical, since at the high

flow rates a unit volume of water is unable to extract enough heat from the ground. So the water finishes the circulation without extracting or absorbing enough energy from the ground which is not desirable.

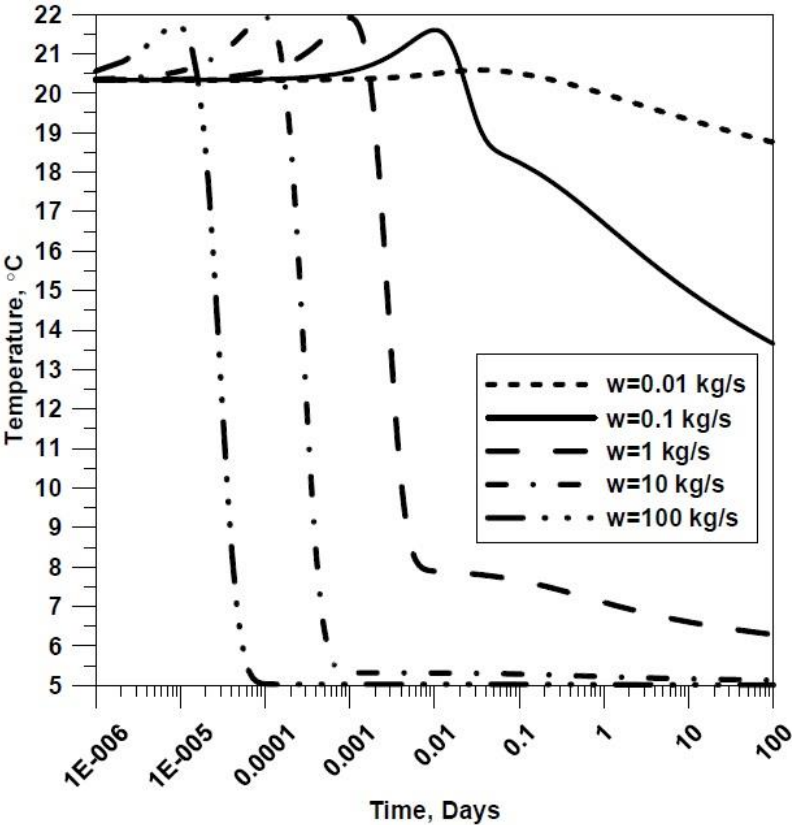


Figure 3.3: Temperature profiles at the exit of the u-tube for various flow rates.

Next, the temperature behavior of the formation are studied at the end of the operation which is 100 days for the various mentioned mass flow rates. As it shown in Figure 3.4 total effected area for the duration of 100 day is approximately around 0.2-12m which are close enough to the borehole and the u tube. As it is shown in the Figure 3.4, temperature difference for the high mass flow rates is significantly larger. Since when mass flow rate is high, more energy can be extracted from the formation by the circulating water. Furthermore, as it is expected that we see a little temperature changes for the lower mass flow rates such as 0.01kg/s since the circulating water can not absorb enough energy from the formation so that the temperature of the formation approximately remains constant. However for flow rates of more than 1 kg/s, the differenes in the temperature profiles are not significant. This is because when the rates are more than 1kg/s, the heat transfer

between the borehole and the reservoir slows down because of the Thermal equilibrium between the circulating water and the formation.

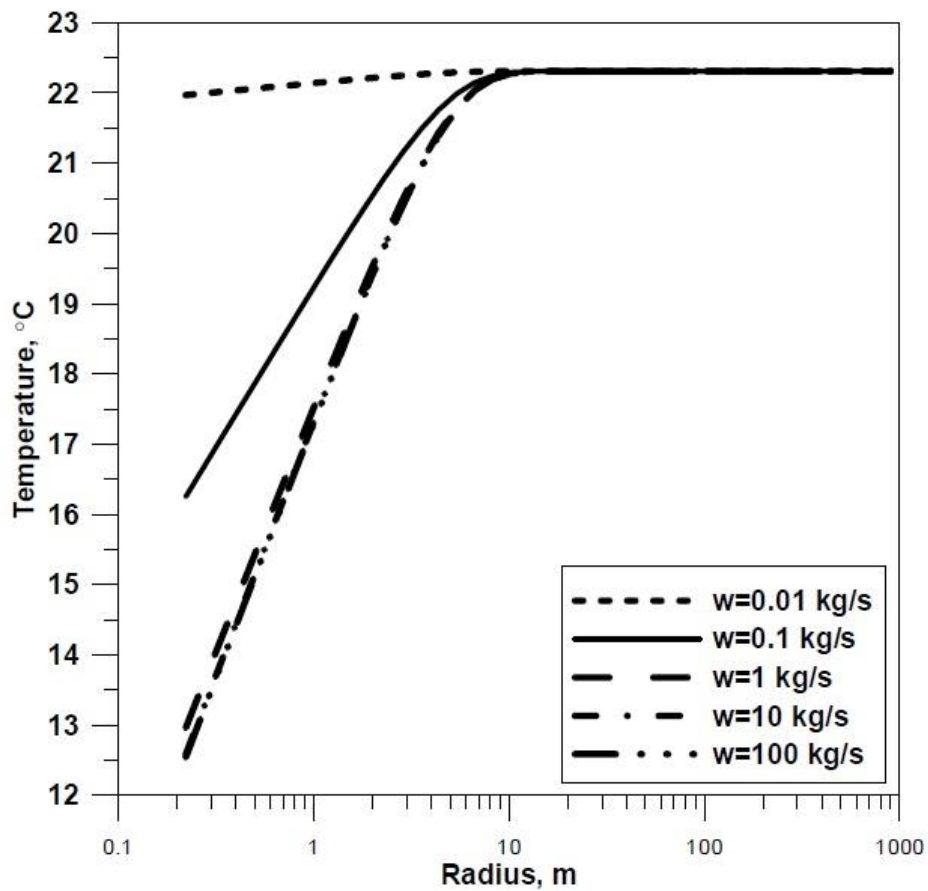


Figure 3.4: Temperature profile of the formation at the 100th day.

The final case that we have studied in the radial system is the presence of underground water flow. When underground water flow is present in the formation, it is usually cooler than what the geothermal gradient would have provided as a temperature distribution for the system. In order to simulate the effects of such cooling, we assumed that the upper 50 m of formation had initial temperatures given by that of the geothermal gradient that is $0.033 \text{ }^\circ\text{C/m}$ which is shown in Table 3.1. The lower 50 m of formation is assumed to bear underground water flow so that the initial temperature is set to be $15 \text{ }^\circ\text{C}$. temperature distribution for this case is shown in figure 3.5. The results are shown in Figure3.6. This figure gives the outlet temperatures profile of the u-tube for two different mass flow rates of 0.1 kg/s and 10 kg/s . When the flow rate is lower (0.1kg/s), the outlet temperatures are affected significantly. As you see two temperature profiles are 0.1kg/s have different decline

ratio. However, when higher flow rates are used (10kg/s), not much difference is observed especially at later times.

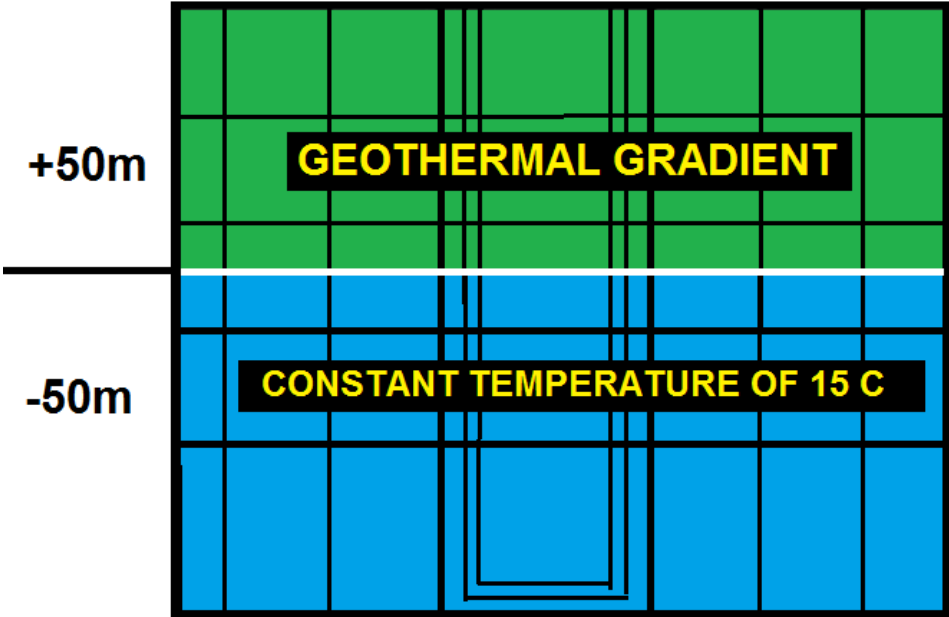


Figure 3.5: Temperature distribution for different initial values.

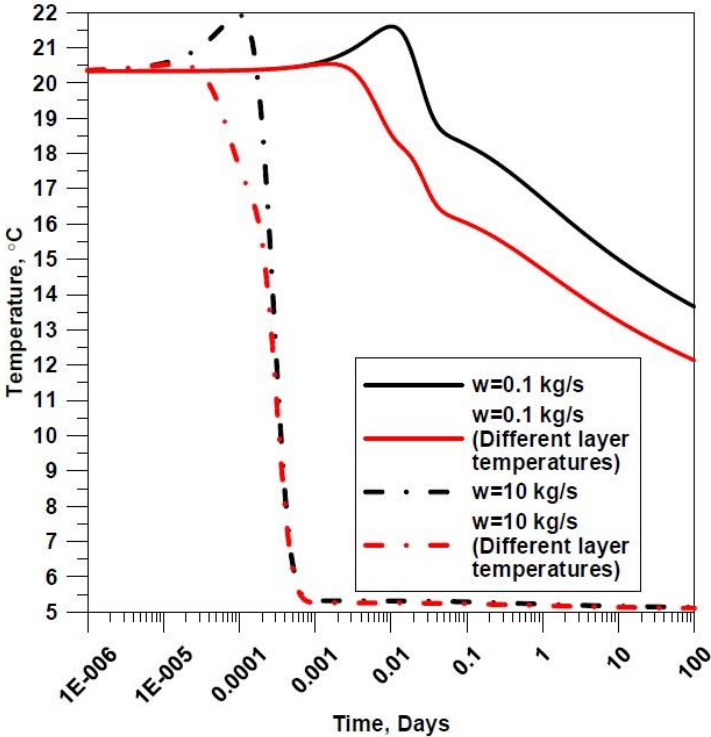


Figure 3.6: Comparison of the production temperature with and without underground water flow for two different mass low rates.

As a result when the flow rates are small, a unit volume of water absorbs more heat during its journey from inlet to outlet of the U-tube so that a change in the formation temperature becomes effective. Also the profile for the different layer temperatures decline more because of cooler temperatures for the formation layer. At higher flow rates, a unit volume of water absorbs little heat by way of conduction because the time it spends in the U-tube is smaller. Hence, the outlet temperature remains unaffected. The changes in the early time for the 10 kg/s curve is because of the different initial temperature distributions.

3.2.2 Cartesian

In this section Cartesian coordinate system will be used in order to investigate the behavior of the GSHPS. The effect of underground water flow is the basic part of study in this section. Furthermore, the effect of thermal conductivity is studied too. The properties of the system for the coordinate system is given in Table 3.2.

Table 3.2: Properties of the system for Cartesian system.

Parameters	Quantity
Surface temperature, °C	20
Radius of borehole, m	0.2
Radius of u-tube, m	0.02
Injection temperature, °C	5
Thermal conductivity of formation, J/(m.s.°C)	2.92
Thermal conductivity of water, J/(m.s.C)	0.6
Density of ground, kg/m ³	2600
Heat capacity of formation, J/(kg.C)	1000
Duration of operation, D	100
Total depth of GSHES in numerical study, m	100
Porosity, fraction	0.1
Total number of grids	620
Geothermal gradient in numerical study, C/m	0.033

The total number of grid blocks used in this part is 620 (11×1×15). The areal grid used for this study is given in Figure 3.7 and Figure 3.8. Figure 3.7 gives the top view of the system and Figure 3.8 gives the front view. A single borehole is located at the center of the system. The grids that are used in this system are assumed to be logarithmic in order to minimize the discretization errors around the borehole.

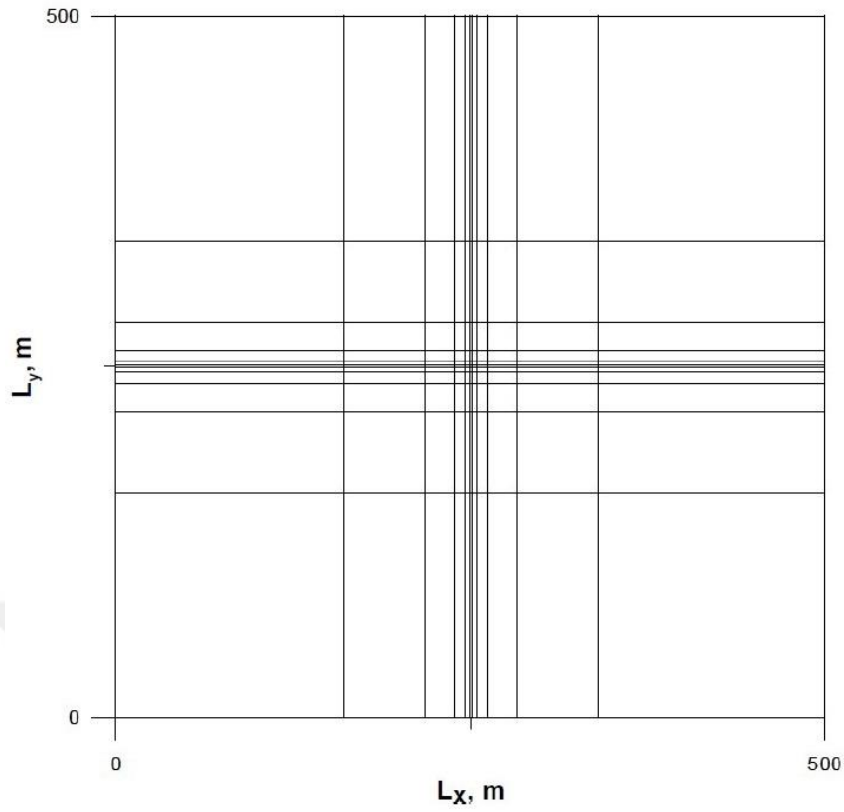


Figure 3.7: Areal logarithmic grid (Top view).

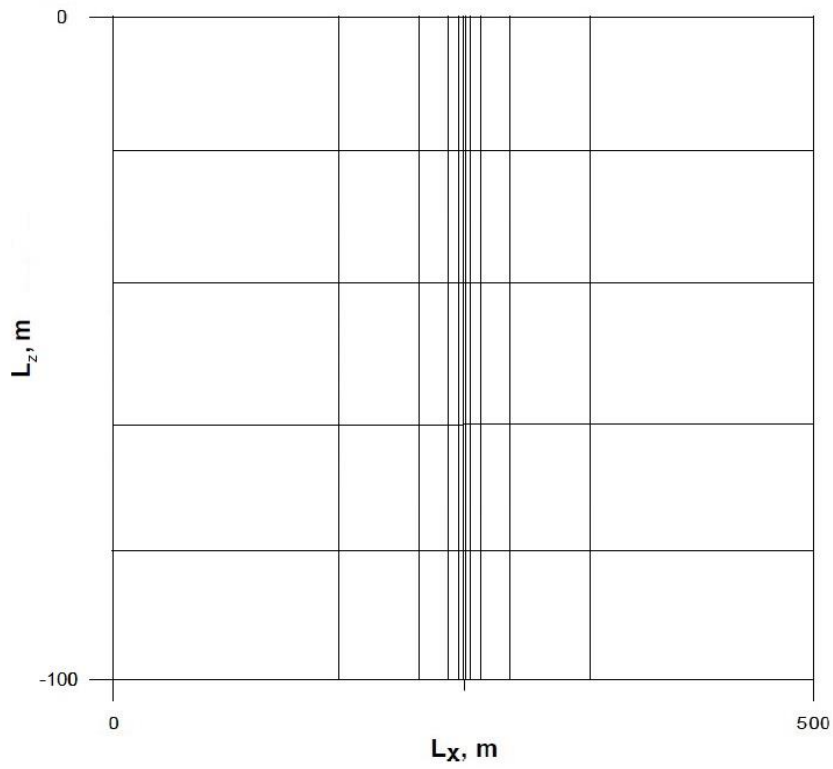


Figure 3.8: Areal logarithmic grid (Front view).

We have studied two case in this section. First, we have assumed underground water flow takes place only in the forth layer from the top and the direction of the flow is assumed to be from left to right. So the initial temperature of the forth layer is assumed to be 15°C and the temperature of the remaining blocks are provided by considering the geothermal gradient.

For analyzing the effects of underground water flow on the performance of the GSHPS the temperature profiles around the well at the end of the operation which is 100 days are studied. Temperature behavior is studied for two different underground mass flow rates. The mass flow rates are 0.0005 and 0.005 kg/m².s. Furthermore, a case without underground flow is added to the profile in order to see the effects obviously.

As mentioned above, a borehole is located in the center of the system so that as expected the effects are reachable at the center of the system.

As shown in the Figure 3.9 when there is no underground water flow the profile turns out to be symmetric as we expect. Since in this case there is no any heat transfer by way of convection and conduction is the only way of heat transferring. By increasing the underground mass flow rate the symmetry destroyed. The temperature of the grid block decreased less because the underground water flow replaces the heat which is transferred to the circulating water in the u tube.

As water flows from the left to the right, the underground water also cools because of the heat transfer to the circulating water. It causes the temperature profile to be smeared on the right of the center, extending the region where temperature changes are observed. On the left side of the well the exact opposite behavior can be seen. On the left the region of changed temperature is brought closer to the well because of the heat support from the underground water movement.

The result of next case that is studied is shown in Figure 3.10. This figure gives the temperature profiles of the forth layer around the well which is bearing the underground water flow at various days. In this case the mass flow rate of 0.005 kg/s.m² is selected for underground water flow.

In this case by increasing the time, as the water is moving from left to right, the temperature is cooled due to the circulating water in the U-tube and the heat transfer from the underground water to the circulating water. Again the cooling takes place

on the right side of the borehole and almost no cooling is observed on the left side again due to the underground water flow. The overall increase in the temperatures of the blocks are caused by conductive heat transfer between the layers especially, the third and the fifth layer. This is due to the fact that a natural state modeling has not been considered for this example and hence the temperatures change slightly away from the borehole.

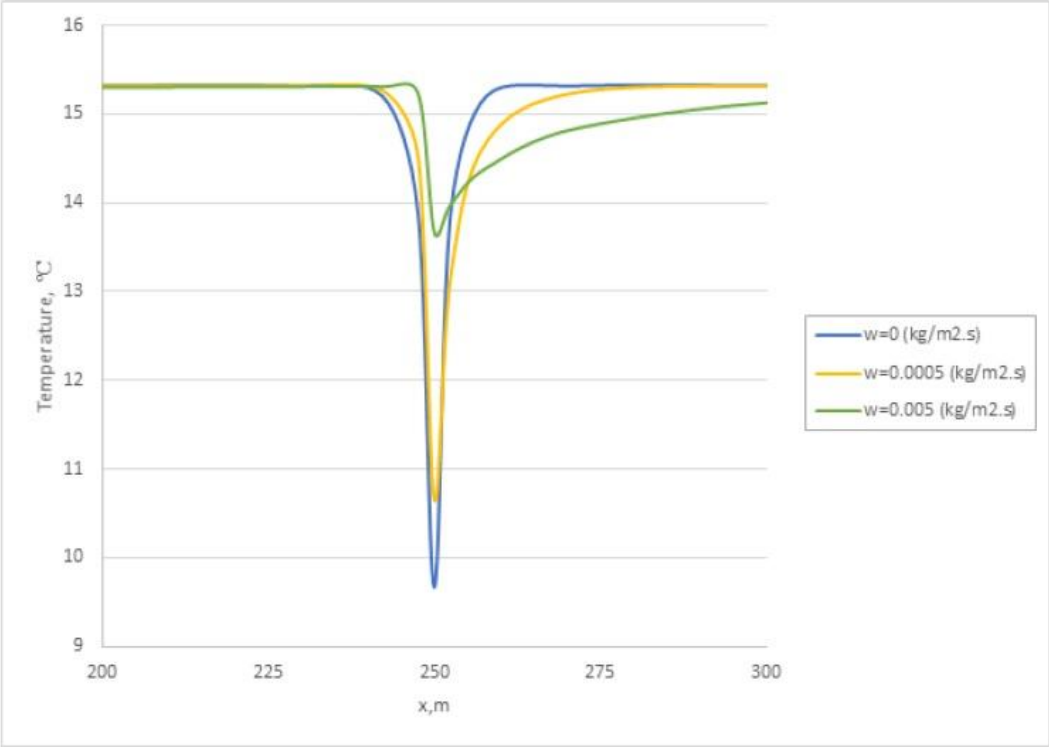


Figure 3.9: Temperature behavior around the well at 100th day for various flow rates.

Finally, Figure 3.11 gives the color map of temperature distribution for the system during the operation. The figure shows the temperature distribution in four different days. As shown, underground water flow in the fourth layer obviously can be seen. Additionally, temperature distribution by considering the geothermal gradient is obvious before starting the operation. By looking closer, the same behavior can be seen around the well in the fourth layer. Our focus was on the fourth layer in previous figures, but this figure gives the total temperature behavior of the system.

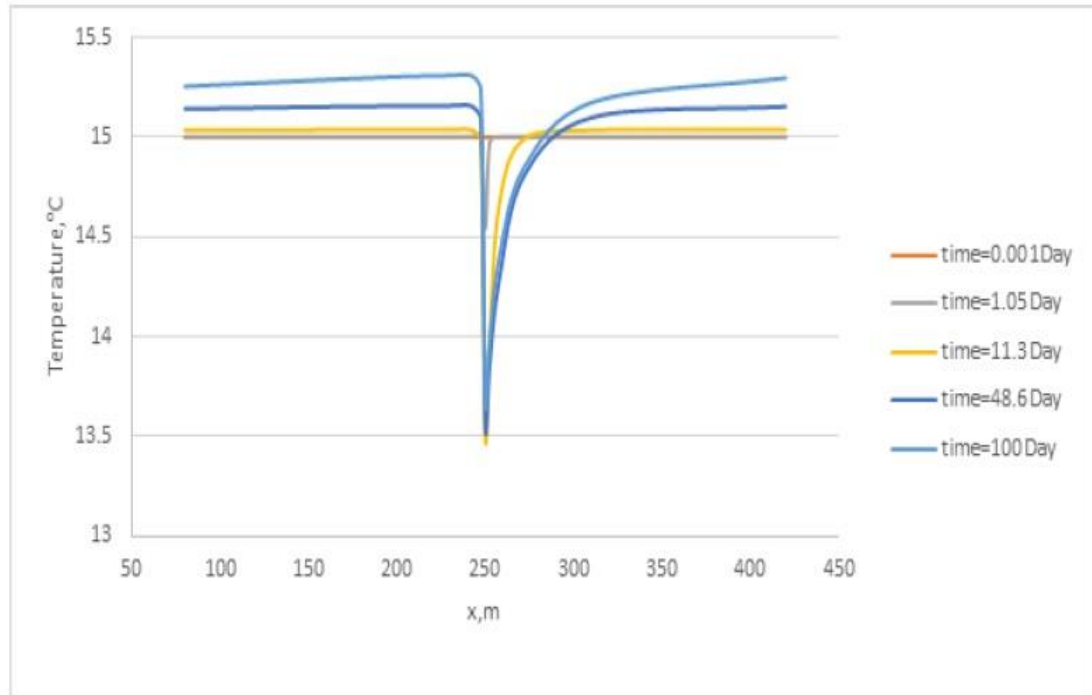


Figure 3.10: Temperature profile around the well for different days and for constant flow rate.

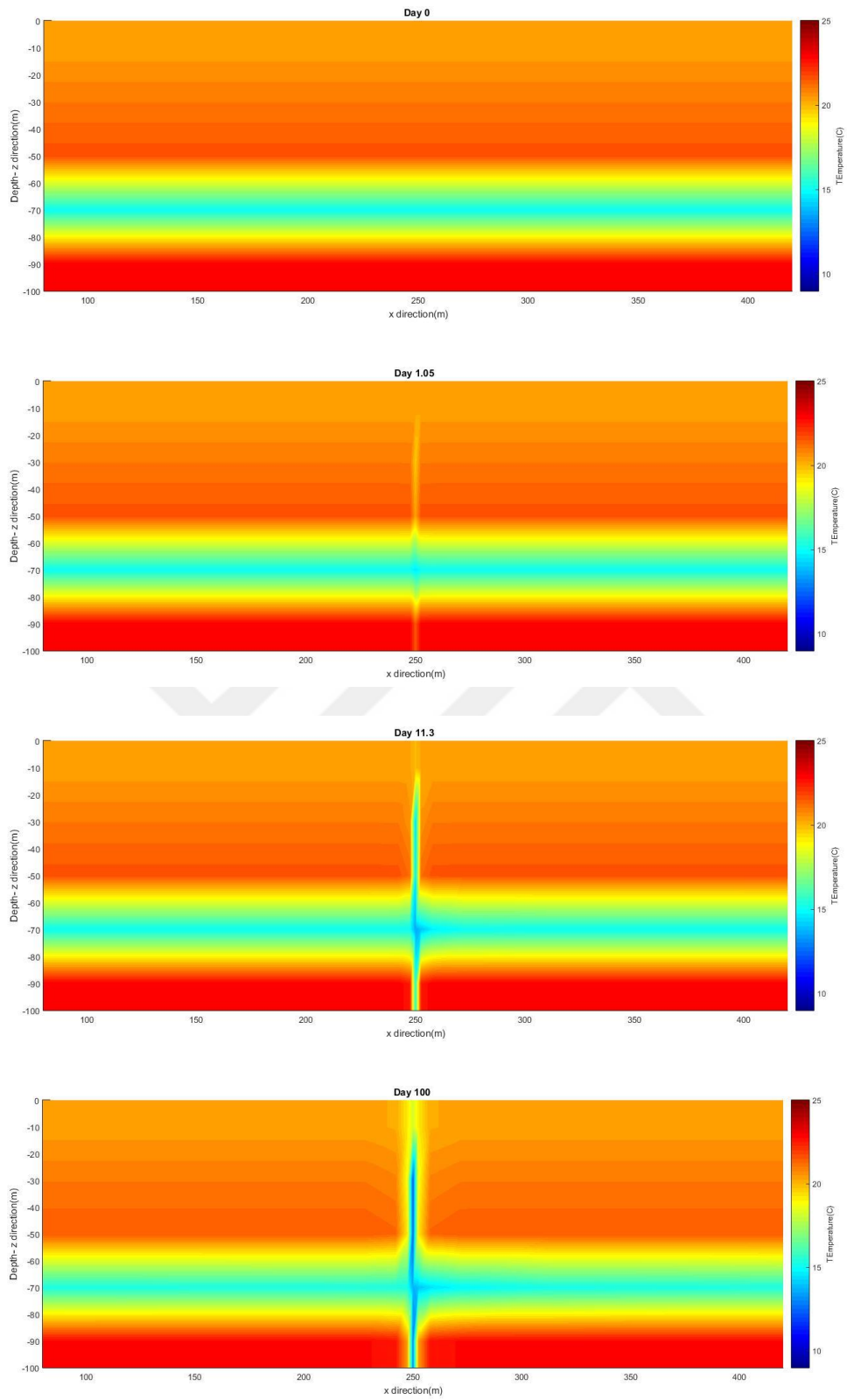


Figure 3.11: Temperature distribution around the well.

In the final case that we consider is the effect of thermal conductivity of the formation on the performance of GSHEs. In order to study this case three different values of the thermal conductivity are used; 1, 2.92 and 4 J/(m.s.°C) for the formation grids. Figure 3.12 and Figure 3.13 show the temperature behavior of the formation for 10th day and 100th day respectively.

As it is clear from Figure 3.12, when the thermal conductivity is low, the borehole is cooled the most since there is little heat transfer among the borehole grids and the formation grids compared with higher cases of thermal conductivity where heat transfer is high among the mentioned grid blocks. Furthermore, as the thermal conductivity is increased, the well is cooled less as it is expected due to the higher heat transfer among the grids of borehole and the formation.

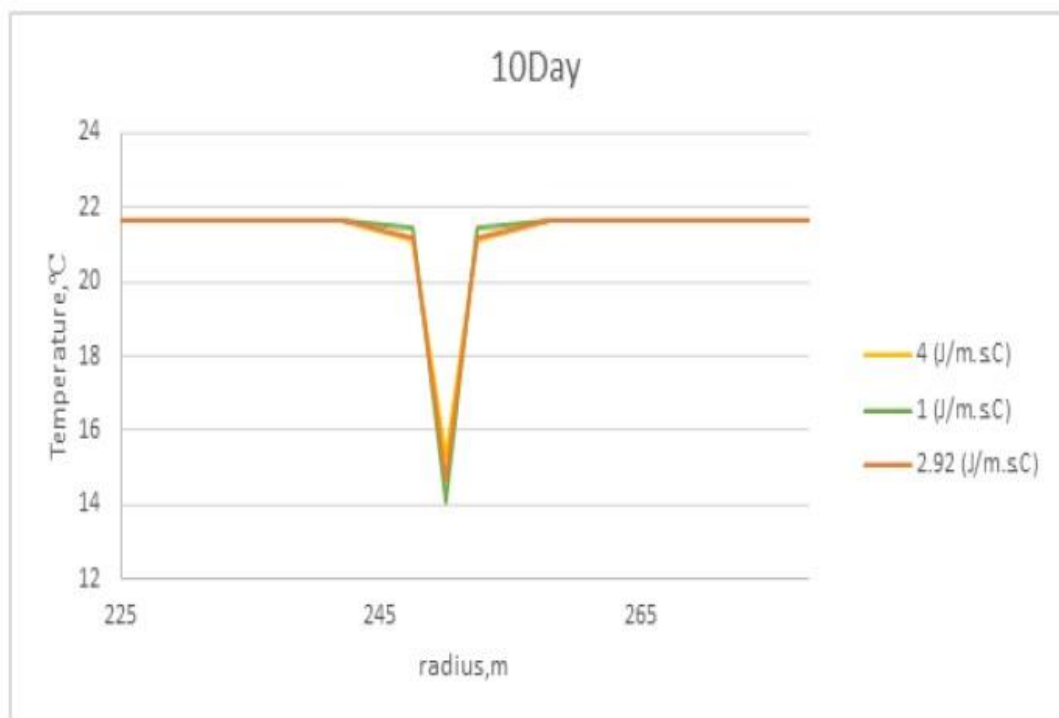


Figure 3.12: The temperature distribution for different formation thermal conductivities at 10th day.

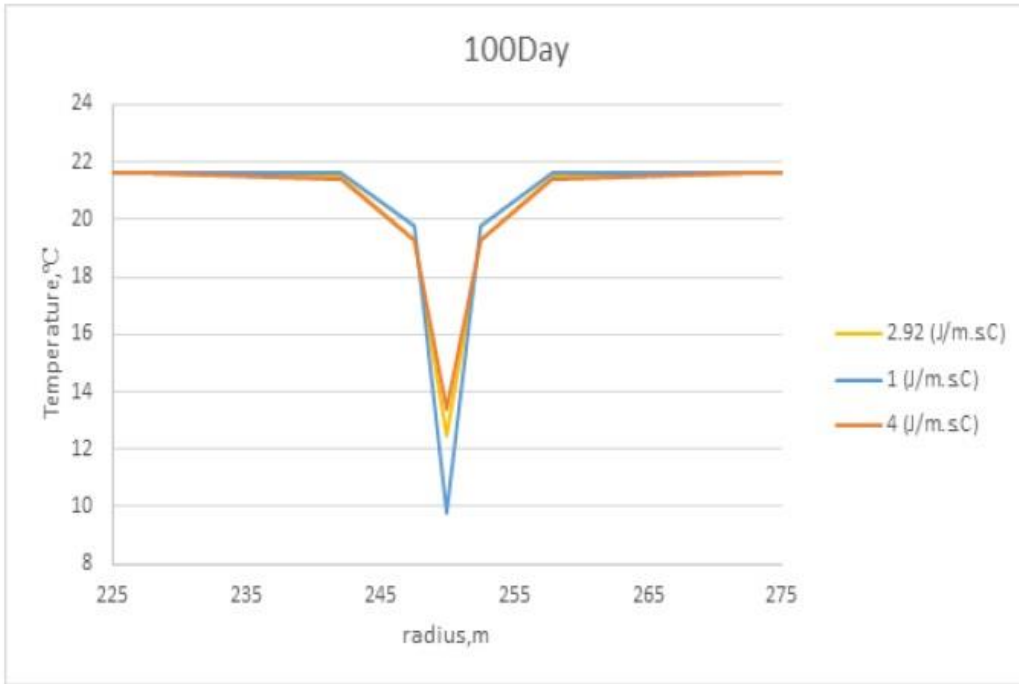


Figure 3.13: The temperature distribution for different formation thermal conductivities at 100th day

4. CONCLUSION

In this study a mathematical model is developed to model the ground source heat exchanger systems. The model is based on solving numerically the energy balance equation. Steady state flow of the fluid is assumed in the model.

Using the model effects of various parameters are analyzed. The parameters considered are: the mass flow rate of the circulating water, the existence and the velocity of underground water flow and the thermal conductivity of the formation.

The following conclusions are obtained:

The results are classified as below:

1. The first case that we studied in the radial system was the effect of mass flow rate of circulating water. As we saw, the flow rate applied to circulating water plays an important role in the amount of heat extracted from the earth. If small flow rates are used, the outlet temperatures decline slowly. As the flow rates increase, the outlet temperature declines faster and at very high rates, the outlet temperature reaches nearly the injection temperature very fast. However, more heat is extracted from the earth in case of higher flow rates.
2. The second case in the radial system was applying different initial temperatures which was different from the temperatures from the geothermal gradient regarding different flow rates. The effects were significant If the flow rate of the circulating water is low. However, as the flow rates increase, this effect is minimized because the convection inside the U-tube dominates the entire process.
3. The first case of Cartesian system was studying the effect of underground water flow on the performance of the GSHES. . By increasing the underground mass flow rate the temperature of the grid block decreased less because the underground water flow replaces the heat which is transferred to the circulating water in the u tube. So high underground water flow significantly affects the temperature distribution in the formation.

4. The last case was studying the effects of thermal conductivity on the performance of the GSHEs. The thermal conductivity of the formation is one of the critical factors that determine the performance of the GSHEs. Lower thermal conductivities lead to more cooling due to lower heat transfer between the borehole and the formation grids and the higher thermal conductivities lead to less cooling because of the higher heat transfer between the borehole and the formation.



REFERENCES

- Akhlaghi, Y. G., Kutun, K., Tureyen, O. I., & Satman, A.** 2015. Effect of Underground Convective Flows on the Performance of Ground Source Heat Exchanger Systems.
- Akhlaghi, Y. G., Tureyen, O. I., & Sataman, A.** 2016. Modeling the temperature behavior of Ground Source Heat Pump Systems. Paper presented at the Stanford Geothermal Workshop.
- Aydin, M., Sisman, A., & Gultekin, A.** 2014. Long Term Performance Prediction of a Borehole and Determination of Optimal Thermal Response Test Duration. Paper presented at the Proceedings.
- Banks, D.** 2009. Thermogeological assessment of open-loop well-doublet schemes: a review and synthesis of analytical approaches. *Hydrogeology journal*, 17(5): 1149-1155.
- Boyd, T. L., Sifford, A., & Lund, J. W.** 2015. The United States of America Country Update 2015. Paper presented at the Proceedings of the World Geothermal Congress.
- Carslaw, H. S., & Jaeger, J. C.** 1959. *Conduction of heat in solids*. Oxford: Clarendon Press, 1959, 2nd ed.
- Cengel, Y.** 2007. *Introduction to thermodynamics and heat transfer+ EES software*: New York: McGraw Hill Higher Education Press.
- Choudhary, A.-u.-R.** 1976. An approach to determine the thermal conductivity and diffusivity of a rock in situ. Oklahoma State University.
- Efficiency, E., & Energy, R.** 2009. *Ground-Source Heat Pumps: Overview of Market Status, Barriers to Adoption, and Options for Overcoming Barriers*.
- EHPA.** 2015. *European Heat Pump Market and Statistics Report 2015 Executive Summary*.
- Gultekin, A., Aydin, M., & Sisman, A.** 2014. Determination of optimal distance between boreholes. Paper presented at the The 39th workshop on geothermal reservoir engineering, February.
- Lund, J., Sanner, B., Rybach, L., Curtis, R., & Hellström, G.** 2004. Geothermal (ground-source) heat pumps—a world overview. *GHC Bulletin*, 25(3): 1-10.
- Lund, J. W., & Boyd, T. L.** 2016. Direct utilization of geothermal energy 2015 worldwide review. *Geothermics*, 60: 66-93.
- Morgensen, P.** 1983. Fluid to duct wall heat transfer in duct system heat storage. Paper presented at the Proc. International Conference on Surface Heat Transfer in Theory and Practice.
- Ozisik, M. N.** 1993. *Heat conduction*: John Wiley & Sons.
- Raymond, J., Malo, M., Tanguay, D., Grasby, S., & Bakhteyar, F.** 2015. Direct utilization of geothermal energy from coast to coast: a review of current applications and research in Canada. Paper presented at the Proceedings World Geothermal Congress, Melbourne, Australia.

- Sanner, B., Hellström, G., Spitler, J., & Gehlin, S.** 2005. Thermal response test—current status and world-wide application. Paper presented at the Proceedings world geothermal congress.
- Sanner, B., Karytsas, C., Mendrinis, D., & Rybach, L.** 2003. Current status of ground source heat pumps and underground thermal energy storage in Europe. *Geothermics*, 32(4): 579-588.
- Signorelli, S., Bassetti, S., Pahud, D., & Kohl, T.** 2007. Numerical evaluation of thermal response tests. *Geothermics*, 36(2): 141-166.
- Sonntag, R. E., Borgnakke, C., Van Wylen, G. J., & Van Wyk, S.** 1998. *Fundamentals of thermodynamics*: Wiley New York.
- Thomas, G. W.** 1982. Exchangeable cations. *Methods of soil analysis. Part 2. Chemical and microbiological properties(methodsofsoilan2)*: 159-165.
- Tureyen, O. I., Onur, M., & Sarak, H.** 2009. A generalized nonisothermal lumped-parameter model for liquid dominated geothermal reservoirs. Paper presented at the Proc. 34th Workshop on Geothermal Reservoir Engineering Stanford University, Stanford, California.
- Wang, H., Qi, C., Du, H., & Gu, J.** 2010. Improved method and case study of thermal response test for borehole heat exchangers of ground source heat pump system. *Renewable energy*, 35(3): 727-733.

CURRICULUM VITAE



Candidate's full name: Yousef Golizadeh Akhlaghi

Place and date of birth: Tabriz, Iran – 31/03/1991

E-mail Address: rasa09.akhlaghi@gmail.com

Education:

B.Sc.: Mechanical Engineering – University of Tabriz

Publications and Presentations on this Thesis:

- **Yousef Golizadeh Akhlaghi**, Omer Inanc Tureyen and Abdurrahman Satman, Modeling the Heat Exchangers Systems , 41th Stanford Geothermal Workshop, Feb 2016 , Stanford University, Stanford, California, USA
- **Yousef Golizadeh Akhlaghi**, Kagan Kutun, Omer Inanc Tureyen and Abdurrahman Satman, Effect of Underground Convective Flows on the Performance of Ground Source Heat Exchanger Systems,40th Stanford Geothermal Workshop, Jan 2015 , Stanford University, Stanford, California, USA.

Other publications and Presentations:

- M.M.Ettefagh, Mobin Alipour, **Yousef Golizadeh Akhlaghi**, Experimental and Theoretical Modelizing of 5MW Offshore Wind Turbine, International Conference on Clean Energy (ICCE 2014), Istanbul, Turkey

- M.M.Ettefagh, Mobin Alipour, **Yousef Golizadeh Akhlaghi**, Experimental and Theoretical Modelizing of 5MW Offshore Wind Turbine with TLP platfrom, International Conference on Acoustic and Vibration (ISAV-2013), Tehran, Iran
- M.M.Ettefagh, Mobin Alipour, **Yousef Golizadeh Akhlaghi**, Modeling of OFFSHORE WIND TURBINE , Special issues of the journals and an edited book by Springer- Renewable Energies

